Synsint Research Group

Available online at www.synsint.com

Synthesis and Sintering

ISSN 2564-0186 (Print), **ISSN** 2564-0194 (Online)

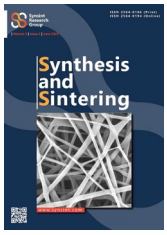

Review article

Synthesis methods and characterization of iron oxide nanoparticles: A biomedical perspective

Saad Ahmed [a,*], **Seema Inayat** [b], **Iram Javed** [c]

[a] *Department of Biological Sciences, International Islamic University Islamabad, Islamabad 44000, Pakistan*
[b] *Aga Khan Centre for Regenerative Medicine and Stem Cell Research, Karachi, Pakistan*
[c] *Department of Chemistry, Division of Science and Technology, University of Education, Lahore, Pakistan*

A B S T R A C T

Iron oxide nanoparticles (IONPs) have emerged as pivotal materials in nanomedicine due to their unique magnetic, catalytic, and biological properties. This review examines a variety of synthesis methods: chemical (co-precipitation, sol-gel, thermal decomposition, microemulsion), physical (ball milling, laser ablation, arc discharge, physical vapor deposition, spray pyrolysis), and biological (plant-mediated, microbial, and biomolecule-assisted) and discusses how these techniques influence nanoparticle size, crystallinity, and surface functionality. We also detail characterization techniques, such as SEM, TEM, XRD, DLS, and FTIR, that are critical for optimizing IONP performance in biomedical settings. Despite considerable progress, issues with reproducibility, scale-up, and biocompatibility remain. Future efforts should focus on standardizing protocols, integrating real-time monitoring, and conducting extensive safety assessments to facilitate the clinical translation and large-scale production of IONPs for diverse applications.

KEYWORDS

Iron oxide nanoparticles
Nanomedicine
Synthesis
Characterization

OPEN ACCESS

1. Introduction

In the 21st century, nanotechnology has evolved and transformed science and technology, unlocking new opportunities for designing materials with unique physical, chemical, and biological properties [1]. Nanoscale materials play a crucial role in biomedicine because of their size compatibility with various biological structures. They are small enough to penetrate cellular environments without disrupting normal functions [2]. They can access areas that other materials cannot, which can induce either the growth or death of cells [3]. Among these nanomaterials, iron oxide nanoparticles (IONPs) have garnered significant attention, particularly in the biomedical field, due to their exceptional magnetic, optical, and catalytic properties [4].

The reactivity of iron, essential for macroscopic applications such as rusting, becomes even more important at the nanoscale. Finely divided iron exhibits pyrophoric behavior at this level, making it highly reactive and challenging to handle [5, 6]. This extreme reactivity initially limited the exploration of iron nanoparticles [7]. However, their potent magnetic and catalytic properties have redirected attention toward their vast potential. Iron oxide nanoparticles, in particular, stand out for their ability to be promptly magnetized under an external magnetic field, undergo self-heating, and exhibit precise movement along magnetic gradients [8].

Iron and oxygen combine chemically to form iron oxides, with approximately 16 distinct compounds identified. Iron (III) oxide, commonly known as rust, is a prevalent form in nature [9]. Iron oxides are abundant, inexpensive, and essential in biological and geological processes [10]. Their nanoscale derivatives, however, pose unique challenges related to stability, biocompatibility, and long-term environmental and health impacts. Addressing these issues requires a deeper understanding of their properties and behavior under diverse conditions [11].

* Corresponding author. *E-mail address:* saad.bsbt1590@iiu.edu.pk (S. Ahmed)
Received 4 April 2025; Received in revised form 10 June 2025; Accepted 17 June 2025.

https://doi.org/10.53063/synsint.2025.52284

The historical development of IONPs as a research focus reveals a gradual shift from fundamental studies on iron chemistry to applications in medicine and diagnostics [12, 13]. IONPs primarily consist of iron oxides such as magnetite (Fe_3O_4), maghemite (γ-Fe_2O_3), and mixed ferrites (MFe_2O_4, where M = Co, Mn, Ni, or Zn) [14]. At the nanoscale, these particles exhibit superparamagnetic behavior, a property that makes them invaluable in biomedical applications [15]. Their strong magnetic moments in an external magnetic field, combined with no residual magnetism when the field is removed, make them suitable for a range of applications. This includes magnetic resonance imaging (MRI), magnetic particle imaging (MPI), hyperthermia therapy, targeted delivery of drugs, proteins, antibodies, and nucleic acids, as well as biosensing, tissue repair, and biomolecule separation [16–25]. This broad range of applications arises from their magnetic properties and the ability to synthesize them in various sizes and shapes. Moreover, nanoparticles have been utilized in various non-biomedical fields, as summarized in Fig. 1.

Fig. 1 demonstrates the multifunctional roles of IONPs in various non-biomedical domains: a) agriculture, where IONPs improve seed priming, act as growth-promoting fertilizers, and offer protection against pests and pathogens [26]; b) environmental Applications, highlighting the use of IONPs for pollutant remediation and water purification through coagulation and contaminant adsorption [27]; c) energy sector, showcasing IONPs in solar cells and batteries [28]; and d) catalysis, emphasizing their applications in acylation, coupling reactions, Fischer-Tropsch synthesis, and catalytic degradation processes [29].

Although iron oxide nanoparticles have significantly contributed to fields such as oncology, regenerative medicine, and molecular imaging, their full clinical potential remains unrealized due to ongoing challenges [4]. Concerns about biocompatibility and safety profiles arise from issues related to cytotoxicity, immune system evasion, and long-term bioaccumulation [30]. While several iron oxide nanoparticles have been evaluated in preclinical and clinical trials, some have even reached the market, and others have been withdrawn due to the emergence of alternative diagnostic probes and protocols (Table 1).

Despite the immense potential of iron oxide nanoparticles, their synthesis and characterization remain critical research areas. These processes directly influence particle size, crystallinity, and scalability, which dictate their biomedical performance. Various synthesis techniques, each with distinct advantages and limitations, have been developed to achieve precise control over these parameters. However, selecting an appropriate synthesis method ensures reproducibility, stability, and functionality. The challenges of scalability and reproducibility present technical barriers that must be addressed to ensure the consistent performance of nanoparticles across batches. These challenges underscore the need for ongoing research into the synthesis, characterization, and application of IONPs.

The rationale for utilizing IONPs for biomedical applications lies in their uniquely favorable convergence of magnetic responsiveness, biocompatibility, and synthetic tunability. Unlike many other nanomaterials, IONPs exhibit superparamagnetism at the nanoscale, allowing them to be guided or activated by external magnetic fields without retaining residual magnetism, thereby minimizing the risk of aggregation in vivo. Furthermore, their surface chemistry enables precise functionalization with drugs, antibodies, or polymers, allowing for targeted therapeutic delivery and molecular imaging with minimal off-target effects. Compared to alternative imaging agents or drug carriers, IONPs offer an exceptional balance of functional performance, safety, and cost-effective synthesis. Therefore, understanding how different synthesis routes and characterization methods impact their physicochemical properties is essential to harnessing their full clinical and translational potential.

This review aims to provide a comprehensive overview of the

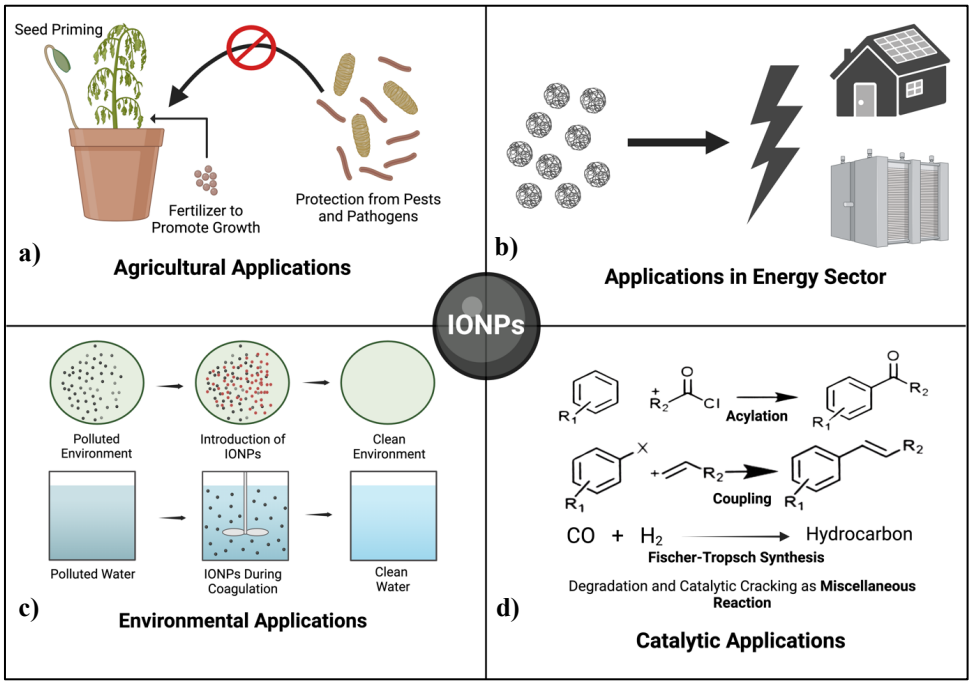

Fig. 1. Diverse non-biomedical applications of iron nanoparticles (IONPs).

Table 1. Clinically relevant iron oxide nanoparticle agents: composition, applications, regulatory status, and withdrawal rationale.

Trade name	Composition	Primary applications	Regulatory status	Reason for withdrawal
Feridex® (Endorem)	Superparamagnetic iron oxide (SPIO); dextran-based	MRI of liver and spleen imaging	FDA-approved (1996); withdrawn (2008)	Decline in demand due to gadolinium-based contrast agents
Resovist®	SPIO coated with carboxydextran	MRI liver imaging; tumor detection	Approved in Europe/Asia; withdrawn (2013)	Commercial viability issues and diagnostic shift toward gadolinium agents
Combidex® (Sinerem)	Ultra-small SPIO (USPIO)	Lymph node imaging; cancer staging via MRI	Clinical trials (never FDA-approved); withdrawn	Funding limitations and competitive pressure from alternative agents
Feraheme® (Ferumoxytol)	USPIO with polyglucose sorbitol carboxymethyl ether	Treatment of iron deficiency anemia in chronic kidney disease	FDA-approved (2009); currently in use	—
Venofer®	Ferric iron sucrose complex	Iron supplementation in anemia	FDA-approved; in current clinical use	—
Clariscan®	Ferumoxytol derivative	MRI contrast for liver and spleen imaging	Approved in select regions (e.g., Europe)	—
SPION-DEX	Dextran-coated SPIO	MRI, targeted drug delivery, magnetic hyperthermia	Preclinical trials	—
AMI-25 (Ferumoxides)	Dextran-coated SPIO	MRI for hepatic lesion detection	FDA-approved (1996); withdrawn	Superseded by agents with improved imaging performance and usability
Nanotherm®	Iron oxide nanoparticles optimized for hyperthermia	Magnetic hyperthermia for cancer treatment	Approved for limited use in Europe (e.g., glioblastoma	—
Ferucarbotran	USPIO stabilized with carboxydextran	MRI liver imaging	Approved in select regions; withdrawn in others	Market competition and the emergence of alternative imaging modalities
Lumirem® (Gastromark)	SPIO coated with silicon dioxide and dextran	MRI contrast for gastrointestinal imaging	FDA-approved; withdrawn	Limited demand in its niche application

synthesis, characterization, and properties of iron oxide nanoparticles, with a particular focus on their biomedical applications. It also examines the challenges associated with their development and application, providing insights into potential solutions and future research directions. By systematically analyzing the current state of knowledge, this review seeks to advance the understanding and optimized design of IONPs, paving the way for their broader application in biomedical sciences.

2. Synthesis of iron oxide nanoparticles

IONPs are a crucial class of nanomaterials due to their exceptional magnetic, catalytic, and physicochemical properties, making them essential in various fields, including biomedicine, environmental remediation, and advanced materials science. Their synthesis method determines their physicochemical characteristics, such as size, morphology, crystallinity, and surface functionality. This section delves into those synthesis methodologies, categorically exploring chemical, physical, and biological approaches while emphasizing their mechanistic foundations, advantages, and limitations.

2.1. Chemical methods

Chemical synthesis methods involve controlled chemical reactions to produce IONPs with specific properties. These techniques are often scalable and versatile, enabling precise control over particle size, morphology, and crystallinity. Fig. 2 provides a detailed schematic representation of the discussed chemical synthesis methods below.

a) co-precipitation, a facile technique involving the simultaneous precipitation of Fe^{2+} and Fe^{3+} salts by the addition of a base (e.g., NaOH, NH_4OH), leading to the formation of IONPs, which are subsequently washed, dried, and ground. b) the sol-gel method is a bottom-up approach based on the hydrolysis and condensation of iron precursors in a solvent, followed by aging and drying under different conditions (supercritical, thermal, or freeze drying) to obtain IONPs with controlled morphology and porosity. c) thermal decomposition method, a high temperature synthesis route where iron precursors decompose in a high-boiling-point organic solvent under an oxygen or inert atmosphere, allowing precise control over nanoparticle size, crystallinity, and monodispersity d) microemulsion method, a colloidal synthesis approach utilizing the controlled mixing of aqueous and organic phases containing iron hydrate salts and a precipitating agent, enabling the formation of monodisperse nanoparticles through nanoscale reactant exchange in stabilized microdroplets.

2.1.1. Co-precipitation method

This technique is one of the simplest and most commonly used for synthesizing IONPs. It involves precipitating iron oxides from an aqueous solution that contains ferric (Fe^{3+}) and ferrous (Fe^{2+}) salts under alkaline conditions [5, 31]. The stoichiometric reaction typically follows this equation:

$$Fe^{3+} + Fe^{2+} + 8OH^- \rightarrow Fe_3O_4 \text{ (magnetite)} + 4H_2O \quad (1)$$

The mechanism begins with the hydrolysis of Fe^{2+} and Fe^{3+} ions, forming intermediate hydroxide species such as $Fe(OH)_2$ and $Fe(OH)_3$ as represented by the reactions below:

$$Fe^{2+} + 2OH^- \rightarrow Fe(OH)_2 \quad (2)$$

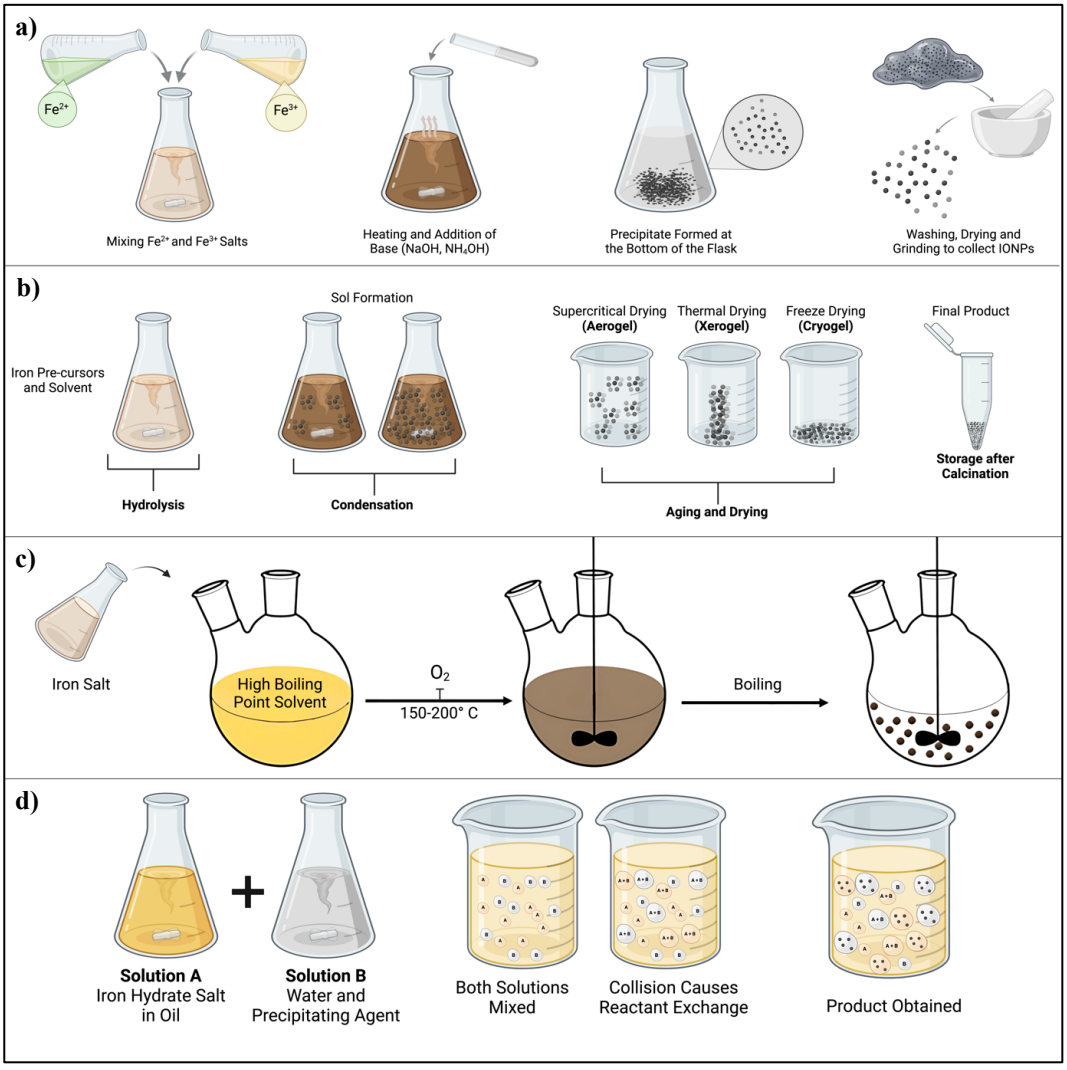

Fig. 2. Four distinct chemical methods for synthesizing iron oxide nanoparticles.

$$Fe^{3+} + 3OH^- \rightarrow Fe(OH)_3 \quad (3)$$

These species undergo nucleation and growth processes, leading to the formation of magnetite (Fe_3O_4) or other iron oxides like hematite (Fe_2O_3) or maghemite (γ-Fe_2O_3) [32].

Key factors influencing this method include pH, temperature, and ionic strength. Maintaining a pH range between 8 and 14 ensures the rapid precipitation of iron hydroxides. Higher temperatures (~80 °C) promote better crystallinity and reduce nanoparticle defects. Due to the presence of additional ions, Ionic strength can affect the zeta potential, ultimately influencing particle agglomeration [33].

Classical nucleation theory can describe the nucleation and growth process [34]. In this theory, the formation of stable nuclei is governed by the change in Gibbs free energy (ΔG), which is influenced by both surface energy (γ) and volume energy (G_v). The total free energy change for the formation of a spherical nucleus of radius is given by [50]:

$$\Delta G(r) = 4\pi r^2\gamma + \frac{4}{3}\pi r^3 G_v \quad (4)$$

The first term ($4\pi r^2\gamma$) corresponds to the surface energy, which increases with the surface area of the nucleus. While the second term ($(4/3)\pi r^3 G_v$) corresponds to the volume energy, which decreases with increasing nucleus size.

The critical radius (r_c) of the nucleus is determined by setting the derivative of $\Delta G(r)$ with respect to r to zero.

$$r_c = -\frac{2\gamma}{G_v} \quad (5)$$

Once the nucleus reaches the critical size r_c, it becomes stable and can grow further by adding solute species from the surrounding solution. Particle growth is often influenced by a phenomenon known as Ostwald ripening, where smaller particles dissolve and redeposit onto larger ones due to differences in chemical potential [34].

The use of surfactants in the co-precipitation method is crucial for stabilizing nanoparticles. Surfactants such as oleic acid or oleylamine bind to the surface of nanoparticles, forming a protective layer that prevents agglomeration and enhances dispersibility [35, 53]. They also influence particle growth by regulating diffusion rates at the nanoparticle-surfactant interface, directly affecting particle size and uniformity [36].

The zeta potential, which reflects the surface charge of nanoparticles, plays a key role in determining the stability of nanoparticle dispersions.

Factors such as ionic strength and surfactant adsorption significantly impact the zeta potential, influencing the overall stability of the nanoparticles in suspension [37]. The stability of the colloidal system can be evaluated using the Derjaguin-Landau-Verwey-Overbeek (DLVO) theory, which considers the balance between attractive van der Waals forces and repulsive electrostatic forces [38].

The total interaction energy (V_T) between the particles is given by [51]:

$$V_T = V_A + V_R \quad (6)$$

When $V_R > V_A$, the nanoparticles remain stable in suspension.

2.1.2. Sol-gel method

The sol-gel method is a widely utilized chemical approach for synthesizing IONPs, offering precise control over particle size, morphology, and crystallinity. This method involves transforming a liquid "sol", a colloidal suspension of particles, into a solid "gel" phase through controlled hydrolysis and condensation of metal precursors [39]. The sol-gel method is particularly advantageous for producing nanoparticles with high purity and uniform composition, making it suitable for various applications such as catalysis, coatings, sensors, and biomedical devices. It also enables the synthesis of mixed-metal oxides, further enhancing its versatility [40].

The sol-gel process typically begins with the hydrolysis of metal alkoxides or inorganic salts, which serve as precursors [41]. Metal alkoxides, such as iron (III) isopropoxide ($C_9H_{21}O_3$), or metal salts, such as iron nitrate ($Fe(NO_3)_3$, are dissolved in a suitable solvent like ethanol or methanol. Water is introduced into the solution, initiating hydrolysis, where metal alkoxides react with water to form metal hydroxides [42].

The general hydrolysis reaction can be written as:

$$M(OR)_n + nH_2O \rightarrow M(OH)_n + nROH \quad (7)$$

In this equation, $M(OR)_n$ represents the metal alkoxide, $M(OH)_n$ represents the metal hydroxide intermediate, and nROH is the alcohol that is released as a by-product. The hydrolyzed metal hydroxides then undergo condensation reactions, where hydroxyl groups react to form metal-oxygen-metal (M–O–M) in bridges [43].

This condensation process leads to the formation of a polymeric network, as shown below:

$$M(OH)_n + M(OH)_n \rightarrow M–O–M + H_2O \quad (8)$$

The solution transitions into a gel, a semi-solid three-dimensional network containing iron hydroxides or oxides dispersed within the solvent [31]. This process marks a key stage in the sol-gel method, and its progression can be influenced by factors such as precursor concentration, solvent type, and reaction conditions. As the gel forms, it is allowed to age, and further condensation reactions occur, leading to structural rearrangement and densification of the gel network. After aging, the gel undergoes drying to remove the solvent and any residual by-products, forming a xerogel (a dry gel). The drying process can be performed under ambient conditions, supercritical conditions (to produce aerogels), or freeze-drying. Once the xerogel is obtained, it is calcinated to decompose organic residues and crystallize the desired iron oxide phase [44]. For example, calcination at moderate temperatures (~300–400 °C) leads to the formation of magnetite (Fe_3O_4), while higher temperatures (~600–800 °C) yield hematite (α−Fe_2O_3) [31].

Reaction parameters strongly influence the final properties of the IONPs synthesized by the sol-gel method. The type of precursor plays a critical role in determining the hydrolysis and condensation rates, which in turn affect particle size and uniformity [45]. While expensive, metal alkoxides offer better control over reaction kinetics than inorganic salts [46]. Another key parameter is the hydrolysis ratio, defined as the molar ratio of water to precursor (H_2O: $M(OR)_n$). A higher hydrolysis ratio accelerates the hydrolysis and gelation processes but can lead to uncontrolled particle growth and agglomeration. Conversely, a lower hydrolysis ratio promotes slower gelation, resulting in smaller, more uniform particles [47]. The pH of the reaction medium also has a significant impact on the sol-gel process. Under acidic conditions, gelation proceeds more slowly, allowing for better control over particle morphology, whereas basic conditions favor rapid gelation and larger particle sizes [48].

Temperature and calcination conditions are equally important in the sol-gel method. Higher reaction temperatures enhance the rate of hydrolysis and condensation, promoting faster gelation. Similarly, the calcination temperature affects the crystallinity, particle size, and phase composition of the final product [49].

2.1.3. Thermal decomposition method

The thermal decomposition method is a highly efficient and widely utilized chemical technique for synthesizing IONPs with controlled size, morphology, and crystallinity. This method involves the thermal breakdown of iron-containing precursors, such as iron carbonyls, acetylacetonates, or iron oleates, at elevated temperatures in the presence of surfactants and organic solvents [52, 53]. The process occurs under an inert atmosphere to prevent unwanted oxidation and produce highly crystalline nanoparticles with uniform size distribution [54].

The thermal decomposition method involves the heating of iron precursors in an organic solvent, leading to the formation of iron oxide nanoparticles. The mechanism typically consists of three main stages: precursor decomposition, nucleation, and growth of nanoparticles.

At elevated temperatures, the iron precursor undergoes thermal decomposition, releasing iron ions (Fe^{2+} and Fe^{3+}) into the solution. For example, the decomposition of iron pentacarbonyl ($Fe(CO)_5$) in a high-boiling-point solvent like octadecene ($C_{18}H_{36}$) is represented by the following reaction [55]:

$$Fe(CO)_5 \rightarrow Fe + 5CO \quad (9)$$

Another common precursor, iron (III) acetylacetonate ($Fe(acac)_3$), decomposes as follows:

$$Fe(acac)_3 \rightarrow Fe^{3+} + 3acac^- \quad (10)$$

After the precursor decomposition, as the concentration of iron ions increases, they aggregate and form small clusters or nuclei [56]. This stage is critical for determining the size and uniformity of the nanoparticles. The nucleation process is the same as the co-precipitation method. Once nucleation occurs, the nuclei grow into larger nanoparticles by adding iron ions and other solute species. The surfactants often influence the growth process in the reaction medium, which regulates the diffusion of solute species to the nanoparticle surface. Surfactants such as trioctylphosphine oxide (TOPO) control particle size and prevent agglomeration [57].

Surfactants are essential in thermal decomposition as they stabilize the growing nanoparticles and control their size and shape. These

molecules bind to the surface of nanoparticles via functional groups such as carboxyl, amine, or phosphine groups, forming a protective layer that prevents agglomeration [58]. For instance, oleic acid binds to the nanoparticle surface through its carboxylic group, while the long hydrocarbon chain provides steric stabilization.

The binding of surfactants can be represented as:

$$Fe_3O_4 + \text{surfactant} \rightarrow Fe_3O_4\ (\text{surfactant}) \quad (11)$$

The surfactant molecules also influence the diffusion rate of iron ions at the nanoparticle-surfactant interface, directly affecting the growth kinetics and final particle size.

Factors such as the precursor type, reaction temperature, surfactant concentration, reaction time, and inert atmosphere influence the final properties of IONPs synthesized via thermal decomposition. Higher temperatures promote faster decomposition rates and better crystallinity, while surfactants regulate particle size and uniformity.

2.1.4. Microemulsion

The microemulsion method is a versatile and efficient chemical approach for IONPs with controlled size, morphology, and surface characteristics [59]. This method utilizes water-in-oil (w/o) or oil-in-water (o/w) emulsions, where the aqueous phase contains metal precursors, and surfactant-stabilized nanodroplets act as confined reaction spaces, also referred to as nanoreactors [60]. The synthesis of nanoparticles occurs within these nanoreactors, with the micelle size dictating the final nanoparticle dimensions. The precise control offered by this method makes it highly suitable for producing monodisperse nanoparticles.

The mechanism of the microemulsion method relies on the thermodynamic stability and dynamic behavior of surfactants at the oil-water interface. The surfactant molecules form micelles (or reverse micelles in w/o systems) with a hydrophilic core (containing the aqueous phase) and a hydrophobic exterior (interacting with the oil phase) [61]. Nanoparticle nucleation and growth occur within the aqueous core of the micelles. The particle size is directly influenced by the micelle diameter, which depends on the surfactant concentration, the water-to-surfactant ratio (W/S), and the type of surfactant used.

The relationship between micelle size and W/S ratio can be approximated by the scaling relation [34]:

$$d \propto (W/S)^{\alpha} \quad (12)$$

where d is the diameter of the nanoparticles, and α is an empirical exponent that depends on the specific system.

The nucleation process in the micelles is governed by classical nucleation theory. After nucleation, growth follows the Ostwald ripening mechanism, where smaller, unstable particles dissolve and redeposit onto larger, energetically favored particles due to differences in chemical potential shown in the equation below [50, 62]:

$$\mu_i = \mu^0 + \frac{2\gamma V_m}{r} \quad (13)$$

where μ_i is the chemical potential of a particle of radius r, μ^0 is the chemical potential of a flat interface, and V_m is the molar volume of the particle.

2.2. Physical methods

Physical methods for synthesizing IONPs provide excellent control over size, morphology, crystallinity, and purity. These methods generally minimize the use of chemical reactants, reducing the risk of contamination and making them ideal for high-purity applications. Below are key physical methods used for synthesis.

2.2.1. Ball milling

Ball milling involves the high-energy mechanical grinding of bulk iron oxide or precursor materials to nanoscale dimensions. This is accomplished through the impact and friction between milling balls and the material within a rotating cylindrical chamber. The process results in fracture and cold welding, which alters the microstructure of the resulting nanoparticles. Various parameters, such as ball size, rotation speed, and milling duration, influence the outcome. The process can produce polydisperse nanoparticles, often necessitating refinement to achieve uniformity [63–65].

2.2.2. Laser abiation

In laser ablation, a high-energy pulsed laser is focused on a target material submerged in a liquid medium. The energy from the laser vaporizes the material, creating a plasma plume. As the plasma cools, nanoparticles condense and precipitate in the liquid. The liquid medium and laser parameters (such as wavelength and pulse energy) affect the size, morphology, and composition of the nanoparticles. Deionized water produces oxide nanoparticles, while organic solvents yield stabilized nanoparticles with reduced oxidation. [66–68].

2.2.3. Arc discharge

Arc discharge occurs when a strong electrical current flows through iron-based electrodes submerged in a liquid medium. The intense heat from the arc vaporizes the electrode material, leading to plasma formation. As this vapor cools, nanoparticles condense and precipitate. The size and shape of these nanoparticles are affected by variables like current intensity, electrode material, and the liquid medium's composition. Additionally, oxygen in the medium encourages the creation of iron oxide nanoparticles [69, 70].

2.2.4. Physical vapor deposition (PVD)

PVD vaporizes an iron precursor in a vacuum or low-pressure environment, causing the vapor to condense into nanoparticles. This process can be accomplished through thermal evaporation, sputtering, or arc discharge. Deposition parameters, such as substrate temperature, vapor pressure, and rate, influence the size, crystallinity, and morphology of the nanoparticles. PVD is frequently employed to produce monodisperse nanoparticles or thin films, particularly in sensor or catalysis applications. [71, 72]

2.2.5. Spray pyrolysis

Spray pyrolysis involves injecting a solution with iron precursors into a high-temperature furnace. The quick evaporation and thermal breakdown of the droplets generate nanoparticles, which are then gathered using filters or deposition substrates. Factors like precursor concentration, spray rate, and furnace temperature influence the size and shape of the particles. This technique allows for continuous production and works well with various precursor solutions, facilitating the creation of mixed-metal oxides or doped nanoparticles [73].

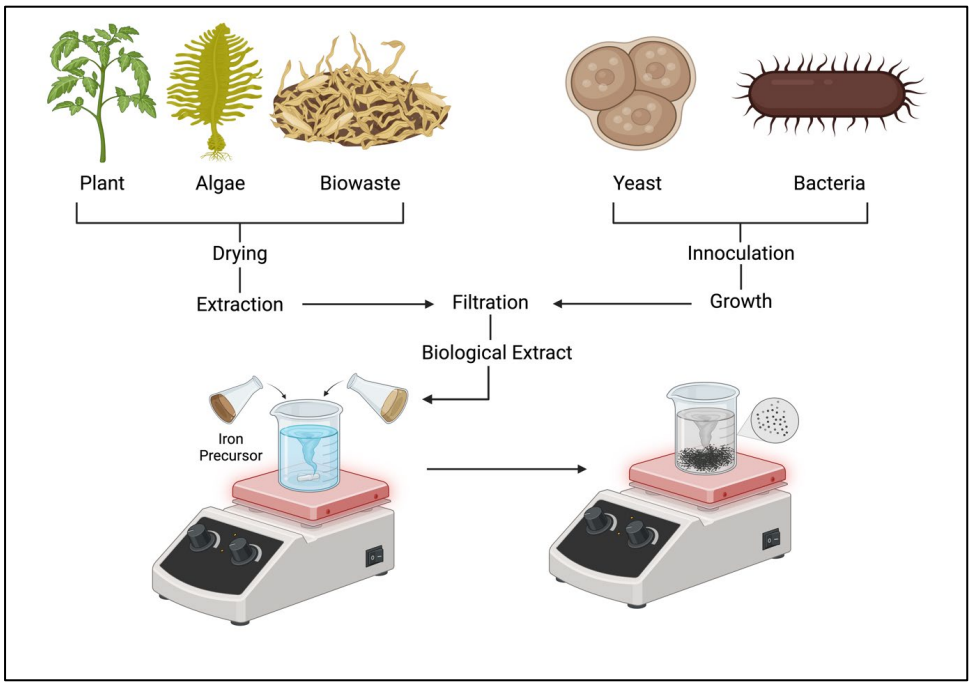

Fig. 3. Green approaches to synthesize iron oxide nanoparticles.

2.3. Biological methods

Green synthesis, also known as biological synthesis, has emerged as an eco-friendly and sustainable approach to producing IONPs. This method utilizes biological systems, including plants, microorganisms, and biomolecules, as natural sources of reducing and stabilizing agents to mediate nanoparticle formation (Fig. 3) [74]. Replacing traditional chemical methods with biological alternatives offers significant advantages, such as reduced environmental impact and the elimination of toxic reagents. This makes green synthesis highly suitable for biomedical applications where safety and functionality are paramount [75].

Fig. 3 illustrates the green synthesis approach for IONPs using biological sources. Plant extracts, algae, and biowaste undergo drying and extraction, while microorganisms (yeast and bacteria) are inoculated and grown to produce biological extracts. These extracts, after filtration, act as reducing and stabilizing agents for the synthesis of IONPs by reacting with an iron precursor under controlled conditions, leading to nanoparticle formation.

2.3.1. Plant-mediated synthesis

Plant-mediated synthesis has gained prominence due to the abundance of secondary metabolites like polyphenols, flavonoids, terpenoids, and alkaloids. These metabolites act as reducing agents, converting iron precursors such as ferric chloride ($FeCl_3$) and ferrous sulfate ($FeSO_4$) into iron oxide nanoparticles [76].

The typical mechanism involves the reduction of Fe^{3+} and Fe^{2+} ions by phytochemicals, followed by the nucleation and growth of nanoparticles. Simultaneously, these metabolites serve as capping agents, stabilizing the nanoparticles by preventing agglomeration. Plant-mediated synthesis generally occurs under mild conditions, such as ambient temperatures or gentle heating, eliminating the need for high-energy inputs or hazardous chemicals. Despite its simplicity and cost-effectiveness, the variability in plant extract composition due to differences in species, growth conditions, and extraction methods can affect the reproducibility of nanoparticle size and morphology [77].

Examples of plants used include Azadirachta indica (Neem), Camellia sinensis (green tea), and Moringa oleifera. These plants have been used to produce IONPs for drug delivery, hyperthermia therapy, and tissue engineering.

2.3.2. Microbial synthesis

Microbial synthesis harnesses the metabolic abilities of bacteria, fungi, and algae to reduce metal ions into nanoparticles [78]. Microorganisms possess unique enzymatic pathways and secrete biomolecules, including reductases, siderophores, and polysaccharides, which facilitate the reduction of iron precursors [79].

Bacteria like Pseudomonas aeruginosa and Bacillus subtilis produce extracellular biomolecules that facilitate the formation of well-dispersed nanoparticles, while species like Shewanella oneidensis can synthesize magnetite nanoparticles under anaerobic conditions. Fungi, such as Aspergillus niger and Fusarium oxysporum, release enzymes and metabolites that yield highly uniform nanoparticles due to their slower metabolic activity. Algae, including Chlorella vulgaris and Spirulina platensis, use their abundant polysaccharide and protein content to reduce and stabilize nanoparticles in aqueous environments, providing excellent biocompatibility [80–82].

Although microbial synthesis allows for precise control over nanoparticle size and morphology, it often requires sterile conditions and careful optimization of metabolic pathways to ensure reproducibility.

2.3.3. Synthesis using biomolecules

Synthesis using biomolecules harnesses the natural properties of proteins, enzymes, polysaccharides, and nucleic acids to mediate the formation of IONPs [83]. Polysaccharides such as chitosan, starch, and cellulose reduce ferric ions and stabilize nanoparticles, enhancing their biocompatibility and biodegradability [84]. This approach is particularly suitable for biomedical applications, including targeted drug delivery and biosensing, due to the excellent functionalization potential of biomolecule-mediated nanoparticles. However, the extraction and purification of these biomolecules can be resource-intensive, and the synthesis parameters require careful optimization to prevent degradation or denaturation [85].

Recent advancements in hybrid green synthesis approaches have combined biological systems with mild chemical methods to enhance efficiency and reproducibility. For instance, microwave-assisted heating of plant extracts accelerates nanoparticle synthesis while preserving the eco-friendly nature of the process [86].

3. Characterization techniques for iron oxide nanoparticles

Characterizing IONPs is a fundamental aspect of nanotechnology research, as it guarantees a thorough understanding of their structure, size, morphology, surface properties, magnetic behavior, and stability [87]. Each characterization method provides insights into specific aspects of the nanoparticles, and collectively, they enable us to tailor IONPs for precise biomedical and industrial applications. This section discusses the principal techniques used to characterize IONPs, emphasizing their underlying physics and the critical parameters they reveal.

3.1. Transmission electron microscopy (TEM) and high-resolution TEM (HRTEM)

TEM provides high-resolution images of IONPs, allowing direct visualization of their size, shape, and morphology. TEM works by transmitting a high-energy electron beam through an ultrathin sample, where electrons interact with the material to produce contrast based on variations in thickness and density [88]. The resolving power of TEM is governed by the de Broglie wavelength of electrons, expressed as:

$$\lambda = \frac{h}{2meV} \tag{14}$$

This equation represents Planck's constant (h), electron mass (m), electron charge (e), and accelerating voltage (V). Higher voltages decrease the electron wavelength, allowing resolutions to reach the atomic scale. TEM is invaluable for revealing their size distribution,

Table 2. Overview of process challenges and scale-up issues for iron oxide nanoparticle synthesis methods.

Synthesis method	Key process challenges	Implications for scale-up and consistency
Co-precipitation	Rapid reaction kinetics with extreme sensitivity to slight variations in operational parameters and chemical additive effects.	Difficulty in maintaining uniform nucleation and growth across batches, leading to variable particle dimensions.
Sol–gel	Multi-stage reactions with interdependent hydrolysis, condensation, drying, and calcination steps that require delicate chemical balance.	Extended processing times and intricate control requirements limit throughput and reproducibility for large-scale production.
Thermal decomposition	High-temperature processing under inert conditions with complex management of organic stabilizers during precursor breakdown.	Elevated energy demands and stringent atmospheric control complicate scale-up, while surface contamination risks affect product uniformity.
Microemulsion	Dependence on a finely tuned balance between surfactant and aqueous phases within confined nanoreactor environments, where slight compositional shifts can alter outcomes.	Limited reactor volumes and high sensitivity to formulation parameters restrict batch size and hinder consistent nanoparticle dimensions.
Ball milling	Mechanical forces that are unevenly distributed, combined with the risk of introducing extraneous contaminants from the milling apparatus.	Inherent variability in particle size and structure complicates quality control and large-scale production reliability.
Laser abiation	Precise energy delivery is required to manage rapid plasma formation and cooling, making the process highly energy-intensive.	Low throughput and sensitivity to laser parameters lead to challenges in achieving reproducible, high-volume synthesis.
Arc discharge	Instabilities in plasma generation and fluctuations in arc conditions, with potential incorporation of electrode-derived impurities.	Inconsistent operating conditions hinder repeatability and scaling, resulting in variability in nanoparticle attributes.
Physical vapor deposition (PVD)	Necessity for ultra-high vacuum systems and exacting control over deposition parameters, with operations highly vulnerable to even minor environmental changes.	High capital costs and operational complexity restrict broad-scale application and consistent deposition over large substrates.
Spray pyrolysis	Synchronization of aerosol generation with rapid thermal decomposition, where droplet dynamics and temperature uniformity are critical.	Variability in droplet behavior under dynamic conditions challenges reproducibility and uniformity in nanoparticle characteristics.
Plant-mediated synthesis	Reliance on naturally derived extracts with inherent variability in bioactive composition and non-standardized processing protocols.	Fluctuations in biomolecule profiles lead to unpredictable reaction dynamics, making consistent large-scale synthesis problematic.
Microbial synthesis	Complex biological regulation requires rigorously controlled, sterile conditions to manage metabolic variations during nanoparticle formation.	Scaling up biological processes is impeded by the sensitivity of microbial systems, resulting in batch-to-batch variability.
Biomolecule-assisted synthesis	Dependence on the quality and stability of extracted biomolecules that are prone to degradation under process conditions necessitates careful handling.	The intensive extraction and stabilization processes, along with variable biomolecule performance, lead to challenges in product consistency.

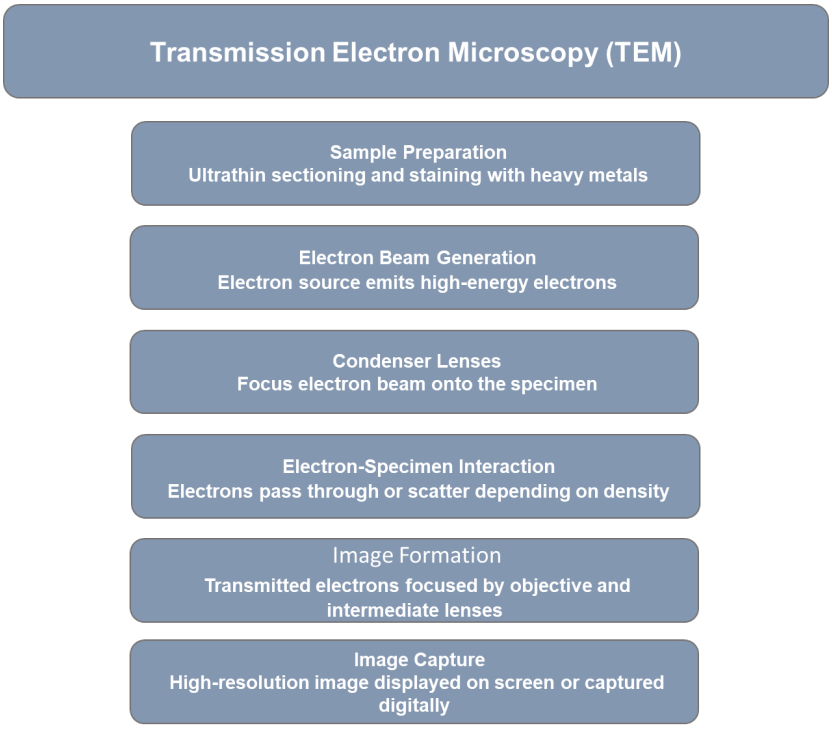

Fig. 4. Transmission electron microscopy (TEM).

agglomeration state, and structural defects of IONPs. High-resolution TEM provides lattice-resolved images, enabling the identification of crystal planes and confirmation of phase purity. Distinguishing between single particles and aggregates is crucial in biomedical applications, as uniform size influences cellular uptake and biodistribution. TEM enables direct measurement of core particle sizes. For instance, Jiang et al. synthesized magnetite (Fe_3O_4) nanoparticles via thermal decomposition and observed monodisperse, quasi-spherical particles with mean diameters of 10 nm, 15 nm, 25 nm, and 40 nm [89]. These particle sizes were tightly distributed, with standard deviations of less than 2 nm in most cases, confirming excellent size control. In another study, Xu et al. reported the synthesis of PEGylated Fe_3O_4 nanoparticles for drug delivery, where TEM revealed a uniform size of ~10 ± 2 nm, suitable for enhanced cellular uptake and in vivo circulation stability [90].

Scanning electron microscopy (SEM), although less commonly used for nanoscale resolution compared to TEM, provides complementary surface topography information, particularly when evaluating agglomerated structures or surface roughness after functionalization [91]. SEM has been employed in green synthesis studies to reveal the surface texture of IONPs capped with plant-derived compounds, which often exhibit a wrinkled or aggregated appearance due to the binding of the organic matrix. Both techniques are usually corroborated with image-based particle size distribution histograms [91].

Nanoparticle size is a significant determinant of biological behavior. TEM-derived sizes below 20 nm are correlated with improved passive targeting via the enhanced permeability and retention (EPR) effect, enhanced internalization by endocytosis, and superparamagnetic behavior, which prevents residual magnetism and aggregation in circulation [14]. For drug delivery and imaging, such size uniformity ensures consistent biodistribution and clearance profiles.

A high-resolution TEM system, illustrating the working principle of TEM through a schematic that depicts electron beam interactions with the specimen, along with a TEM image of nanoparticles showcasing their nanoscale morphology.

3.2. X-ray diffraction (XRD)

XRD is fundamental for determining the crystallinity, phase composition, lattice parameters, and crystalline grain size of IONPs [91]. This technique is based on the diffraction of X-rays from the crystal lattice planes of a material, which Bragg's law can describe:

$$n\lambda=2d\sin\theta \tag{15}$$

Here, λ is the wavelength of the X-rays, d is the interplanar spacing, θ is the angle of incidence, and n is an integer representing the diffraction order.

In typical Fe_3O_4 nanoparticles, the XRD pattern displays characteristic Bragg peaks at $2\theta \approx 30.1°$, $35.4°$, $43.1°$, $53.4°$, $57.0°$, and $62.6°$, corresponding to the (220), (311), (400), (422), (511), and (440) crystal planes of the spinel structure, matching the JCPDS card no. 19-0629 [92].

For IONPs, XRD is beneficial in identifying different phases, such as magnetite or maghemite, as their diffraction patterns exhibit distinct peak positions and intensities. Furthermore, the average crystallite size can be estimated using the Scherrer equation:

$$D=\frac{K\lambda}{\beta\cos\theta} \tag{16}$$

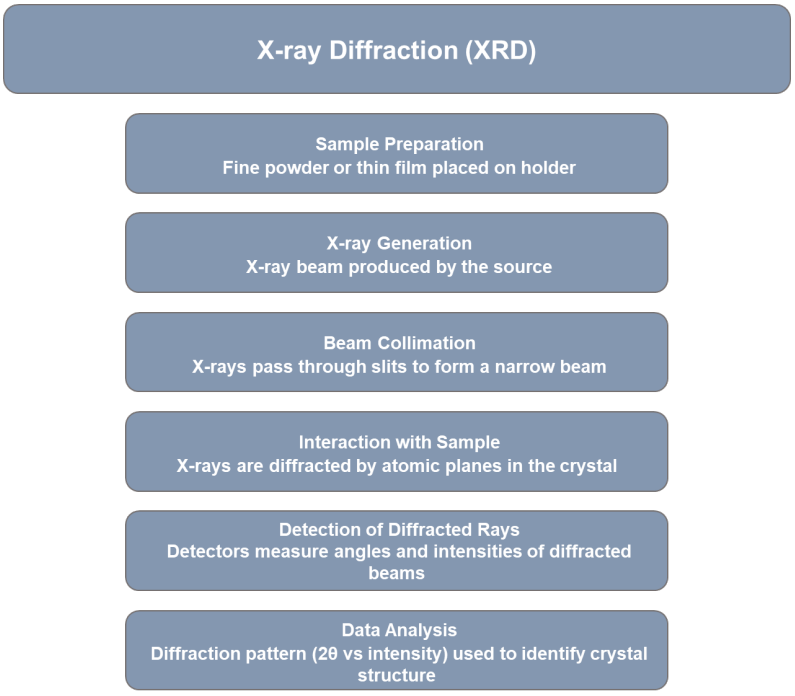

Fig. 5. X-ray diffraction (XRD) analysis.

where D is the crystallite size, K is a shape factor (commonly taken as 0.9), β is the full width at half maximum (FWHM) of the diffraction peak, and θ is the Bragg angle.

Crystallinity and phase identity influence the magnetic and chemical behavior of IONPs. Magnetite offers a higher saturation magnetization compared to maghemite or hematite, making it more effective in MRI and hyperthermia applications. Smaller crystallite size can also enhance surface reactivity, which benefits drug loading and functionalization [93].

Schematic representation of the XRD working principle showing X-ray interaction with the sample, and XRD pattern depicting diffraction peaks corresponding to different crystalline planes.

3.3. Dynamic light scattering and zeta potential (DLS)

DLS is a powerful technique for determining the hydrodynamic diameter of nanoparticles in suspension. It measures the Brownian motion of particles by analyzing fluctuations in the intensity of scattered light over time [94]. The hydrodynamic diameter (d_h) is related to the diffusion coefficient (D) through the Stokes-Einstein equation:

$$d_h = \frac{k_B T}{3\pi\eta D} \tag{17}$$

Here, k_B is Boltzmann's constant, T absolute temperature, and η is the viscosity of the medium.

Unlike TEM, which measures the physical size of the core, DLS provides an ensemble average of the hydrodynamic size, which includes the core, surface coatings, and any adsorbed layers of solvent molecules. This distinction makes DLS particularly useful for analyzing the stability of colloidal dispersions and the effectiveness of surface functionalization. For example, an increase in hydrodynamic size upon adding PEG coatings confirms successful functionalization, which is essential for improving the biocompatibility of IONPs [95].

The zeta potential quantifies the surface charge of nanoparticles and serves as an indicator of electrostatic repulsion between particles in suspension. Generally, a zeta potential of ±30 mV or higher is considered necessary for colloidal stability. Wahajuddin and Arora found that citrate-capped IONPs had a zeta potential of -42 mV, resulting in excellent electrostatic stabilization in aqueous media [14]. Such surface charge profiles are pivotal in predicting interactions with serum proteins and cellular membranes, which in turn affect in vivo performance.

DLS instrument, Working principle involving laser scattering and correlation, Particle size distribution graph indicating nanoscale measurement.

3.4. Fourier transform infrared spectroscopy (FTIR)

FTIR is employed to analyze the surface chemistry of IONPs by identifying functional groups and chemical bonds. FTIR measures the absorption of infrared radiation, which induces vibrational transitions in molecular bonds [96]. The vibrational frequency (ν) of a bond can be calculated as:

$$\nu = \frac{1}{2\pi}\sqrt{\frac{k}{\mu}} \tag{18}$$

For IONPs, FTIR can detect Fe-O stretching vibrations at approximately 530 cm^{-1} and characteristic peaks related to organic capping agents or surface modifiers. For instance, peaks around 1730 cm^{-1} indicate the presence of carbonyl groups, while broad bands near 3400 cm^{-1} suggest the presence of hydroxyl groups [97].

Functionalization of IONPs significantly alters the FTIR spectrum. For example, PEGylated Fe_3O_4 nanoparticles display additional peaks: a broad O–H stretching vibration at ~3400 cm^{-1}, C–H stretching vibrations at ~2920 cm^{-1}, and strong carbonyl (C=O) absorptions at ~1630–1740 cm^{-1}, indicating the successful grafting of PEG or

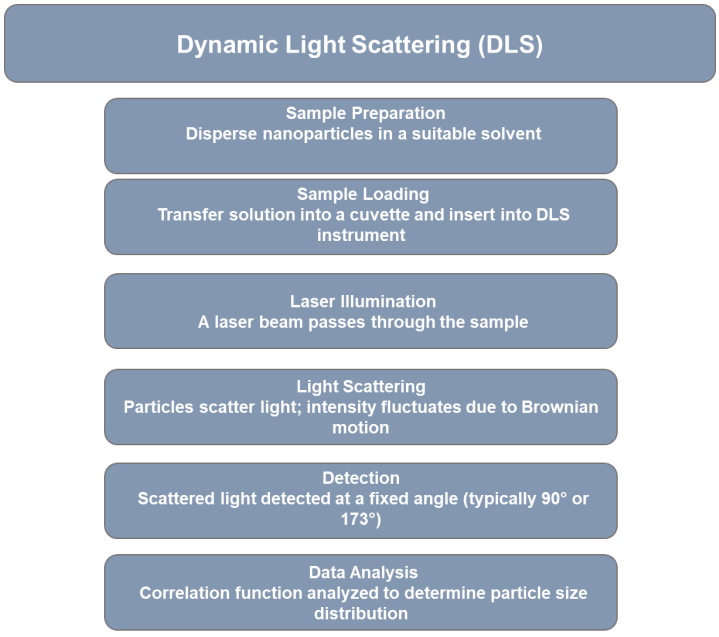

Fig. 6. Dynamic light scattering (DLS) for nanoparticle size analysis.

carboxylic acid-containing ligands. Similarly, nanoparticles capped with plant extracts often exhibit aromatic C=C stretches near 1600 cm^{-1} and –OH or $–NH_2$ groups from biomolecules [98].

In one study, green-synthesized IONPs using Azadirachta indica (Neem) leaf extract exhibited prominent bands at 3435 cm^{-1} (–OH), 1635 cm^{-1} (C=O), and 578 cm^{-1} (Fe–O), confirming both the presence of organic functional groups and the iron oxide core [99]. These surface functionalities influence colloidal stability, cellular uptake, and the ability to conjugate therapeutic agents.

FTIR instrument used for molecular analysis, Schematic representation of the FTIR working principle illustrating infrared absorption by molecular bonds, and FTIR spectrum showing characteristic peaks corresponding to functional groups in the sample.

3.5. Vibrating sample magnetometry

VSM measures the magnetic behavior of IONPs by detecting the magnetic moment induced when the sample vibrates in a uniform magnetic field. The generated signal is proportional to the magnetization of the sample [100]. This technique provides essential parameters, including saturation magnetization (M_s) remanence, and coercivity (H_c).

The magnetization curve obtained from VSM analysis follows the equation:

$$M = M_s\left(1 - \frac{1}{\chi(H+H_c)}\right) \tag{19}$$

Here, M is magnetization, H is the applied magnetic field, and χ is magnetic susceptibility.

For IONPs, superparamagnetic behavior is observed due to their nanoscale size, characterized by negligible remanence and coercivity in the absence of an external field. This property ensures that IONPs do not retain magnetization after removing the magnetic field, a critical feature for preventing aggregation and achieving precise magnetic targeting in vivo for biomedical applications [101].

High saturation magnetization enhances MRI contrast and magnetic heating efficiency in hyperthermia therapy. Superparamagnetic IONPs with low H_c and M_r are safer in biological systems because they minimize magnetic clumping and improve circulation stability [102]. Therefore, optimizing magnetic properties through control of size and synthesis is essential for developing effective nanomedicines.

3.6. Zeta potential analysis

Zeta potential measures the surface charge of IONPs in suspension, providing insights into their colloidal stability. It is derived from the electrophoretic mobility of particles under an electric field, as described by:

$$\zeta = \frac{u\eta}{\varepsilon} \tag{20}$$

where u is the electrophoretic mobility, η is the dynamic viscosity, and ε is the dielectric constant.

For IONPs, a high zeta potential (typically > ±30 mV) indicates good colloidal stability, as the strong surface charge prevents particle aggregation. This property is critical for biomedical applications, where stable dispersions are required in physiological media [37].

VSM instrument used for magnetic characterization, Schematic representation of the VSM working principle illustrating the vibration of the sample in a magnetic field, and Magnetic hysteresis loop depicting the magnetic properties of the material.

Schematic representation of the zeta potential measurement principles, and zeta potential graph depicting particle size and surface charge stability.

3.7. UV-Vis spectroscopy

UV-Vis spectroscopy provides information on the optical properties of IONPs, including ligand-to-metal charge transfer (LMCT) transitions and bandgap energy [103]. For IONPs, absorption peaks typically

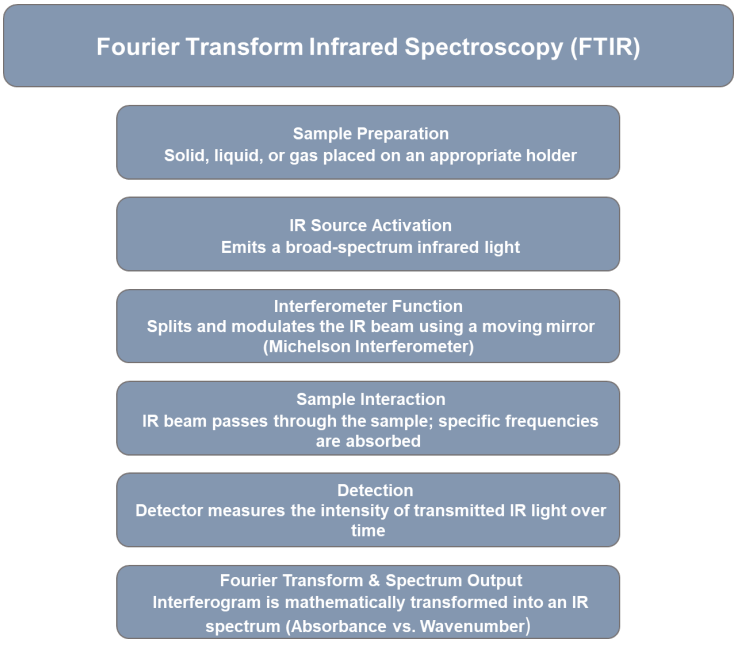

Fig. 7. Fourier transform infrared spectroscopy (FTIR).

occur in the 200–300 nm range, corresponding to electronic transitions in Fe–O bonds. Bandgap energy (E_g) can be calculated from the Tauc plot:

$$(\alpha h\nu)^n = A(h\nu - E_g) \quad (21)$$

where α is the absorption coefficient, hν is the photon energy, and A is a proportionality constant that depends on the type of electronic transition. UV-Vis spectra are also helpful in monitoring surface modifications, as coatings often shift or broaden absorption peaks.

IONPs are characterized by a multifaceted approach to understand their physicochemical, structural, and functional properties. While techniques such as TEM, XRD, and FTIR provide critical insights into morphology, crystallinity, and surface chemistry, advanced methods offer complementary information on surface composition, porosity, and atomic-level magnetic behavior. These techniques are valuable for exploring nanostructural organization and local electronic environments. Together, these methods enable a comprehensive grasp of IONPs, facilitating their optimization for diverse applications in

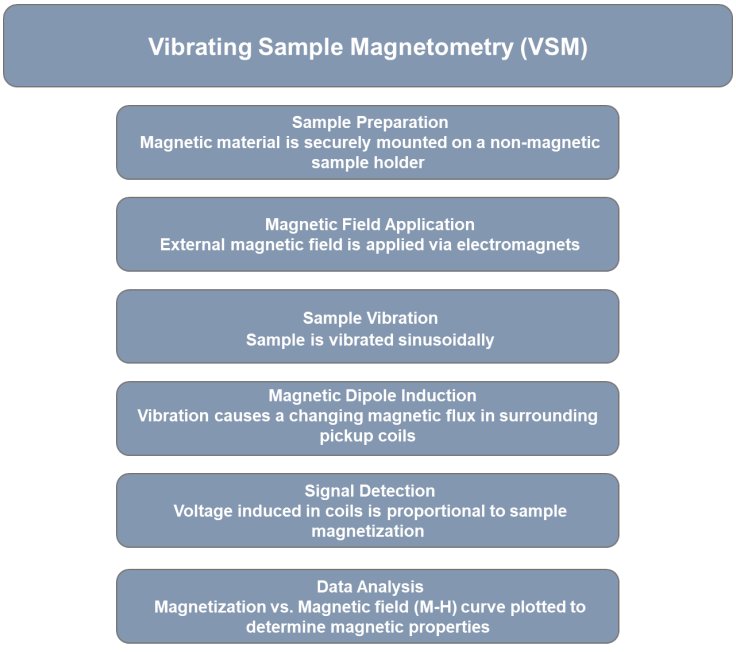

Fig. 8. Vibrating sample magnetometry (VSM).

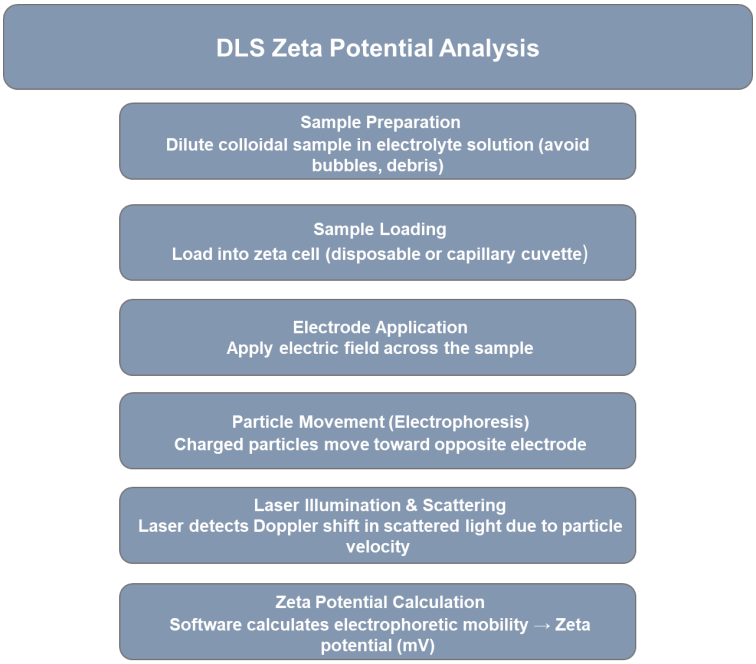

Fig. 9. Zeta potential analysis.

biomedicine, catalysis, and environmental remediation. A summary of these advanced techniques, their principles, and their specific applications in IONP characterization is provided in Table 3.

UV-Vis spectrophotometer used for optical characterization, Schematic representation of the UV-Vis working principle illustrating light absorption by a sample, and UV-Vis absorption spectrum showing characteristic peaks corresponding to electronic transitions in the material.

Fig. 11 shows a) scanning electron microscopy (SEM) for surface morphology analysis, b) thermogravimetric analysis (TGA) for thermal stability assessment, and c) atomic force microscopy (AFM) for nanoscale surface topography evaluation.

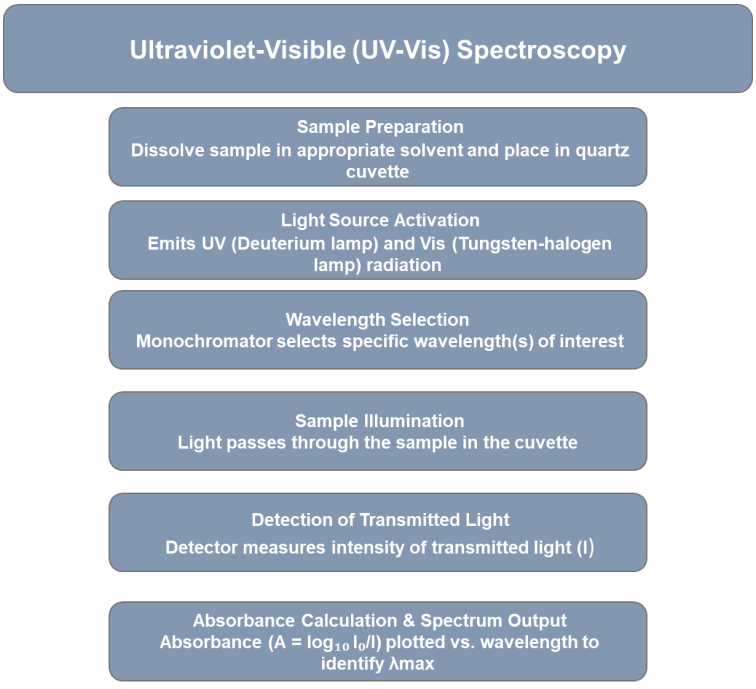

Fig. 10. Ultraviolet-visible (UV-Vis) spectroscopy.

Table 3. Advanced techniques in iron oxide nanoparticles characterization.

Technique	General principle	Key information obtained	Applications
XPS (X-ray Photoelectron Spectroscopy)	Measures the energy of photoelectrons emitted from a material exposed to X-rays.	Surface elemental composition, oxidation states, and chemical bonding.	Determines surface chemistry, oxidation states of iron (Fe^{2+}/Fe^{3+}), and presence of coatings or ligands.
EDS (Energy-Dispersive X-ray Spectroscopy)	Detects X-rays emitted from a sample when excited by an electron beam.	Elemental composition and distribution.	Confirms the presence of iron and other elements (e.g., oxygen, dopants) in IONPs.
BET (Brunauer-Emmett-Teller) Analysis	Measures gas adsorption on a solid surface to determine surface area.	Specific surface area, pore size, and porosity.	Evaluates surface area, which influences reactivity, drug loading, and catalytic properties of IONPs.
TGA (Thermogravimetric Analysis)	Measures weight changes in a sample as a function of temperature.	Thermal stability, decomposition temperatures, and composition of organic/inorganic phases.	Quantifies organic coatings, surfactants, or stabilizers on IONP surfaces.
SAXS (Small-Angle X-ray Scattering)	Analyzes X-ray scattering at low angles to probe nanostructures.	Size, shape, and spatial arrangement of nanoparticles in solution or solid state.	Provides insights into aggregation, interparticle distances, and structural organization of IONPs.
XAS (X-ray Absorption Spectroscopy)	Measures X-ray absorption near the edge structure (XANES) and extended fine structure (EXAFS).	Local electronic structure, coordination environment, and oxidation states.	Probes the local environment of iron atoms, including coordination number and bond distances.
AFM (Atomic Force Microscopy)	Uses a cantilever with a sharp tip to scan surfaces and measure forces.	Topography, surface roughness, and mechanical properties.	Maps surface morphology and measures nanoscale mechanical properties of IONPs.
Mössbauer Spectroscopy	Detects nuclear gamma resonance to study hyperfine interactions.	Oxidation states, magnetic properties, and crystal structure.	Identifies iron phases (e.g., magnetite, maghemite) and quantifies magnetic behavior at the atomic level.

3.8. Integrated contributions of characterization techniques

The characterization of iron oxide nanoparticles relies on a suite of techniques, each contributing distinct yet complementary insights to form a complete picture. High-resolution imaging tools like TEM and HRTEM provide the foundational understanding of size, shape, and crystallinity. While TEM reveals the overall morphology and distribution of the particles, HRTEM delves into the atomic arrangement, ensuring that the synthesized nanoparticles exhibit the desired phase purity and structural integrity.

In parallel, techniques such as XRD play a critical role in verifying the crystalline structure and phase composition through diffraction patterns and estimating crystallite size. These methods validate the visual findings from electron microscopy, bridging the gap between microstructural imaging and crystallographic analysis. DLS further augments this understanding by measuring the hydrodynamic diameter in suspension, which includes the effects of surface coatings and surrounding solvent layers, which is a key factor in predicting behavior in biological environments.

Surface chemistry is equally vital for the functionality and stability of nanoparticles. FTIR identifies functional groups and confirms the presence of capping agents or surface modifiers that stabilize the particles and facilitate further functionalization for biomedical applications. Complementary to these, zeta potential measurements provide a quantitative assessment of colloidal stability by evaluating surface charge, ensuring that the nanoparticles remain well-dispersed and avoiding aggregation under physiological conditions.

Magnetic and optical properties are central to the application of iron oxide nanoparticles in areas such as magnetic resonance imaging and hyperthermia therapy. VSM measures key magnetic parameters, including saturation magnetization, coercivity, and remanence, thereby confirming the superparamagnetic behavior essential for biomedical use. On the other hand, UV-Vis spectroscopy sheds light on the optical and electronic properties, monitoring changes in absorption that may result from surface modifications or electronic transitions within the nanoparticle matrix.

Advanced analytical techniques such as XPS, EDS, BET analysis, and TGA further extend this comprehensive characterization. These methods provide deeper insights into elemental composition, surface area, porosity, and thermal stability, enhancing the overall understanding of nanoparticle performance and guiding the optimization of synthesis protocols.

Together, these integrated techniques create a multidimensional framework that validates the synthesis of iron oxide nanoparticles and precisely characterizes every critical structural and morphological parameter attributed to surface chemistry and magnetic properties. This approach enables researchers and practitioners to fine-tune the nanoparticles for specific applications, ensuring consistency, reliability, and enhanced performance in biomedical and technological settings.

4. Challenges and future Directions

The field of IONPs has seen significant advancements in recent years, yet several critical challenges remain that hinder their clinical and industrial applications. Overcoming these challenges requires a comprehensive understanding of synthesis methods, nanoparticle characterization, safety considerations, and the regulatory hurdles associated with them. Each aspect is intricately linked and must be addressed through multidisciplinary efforts.

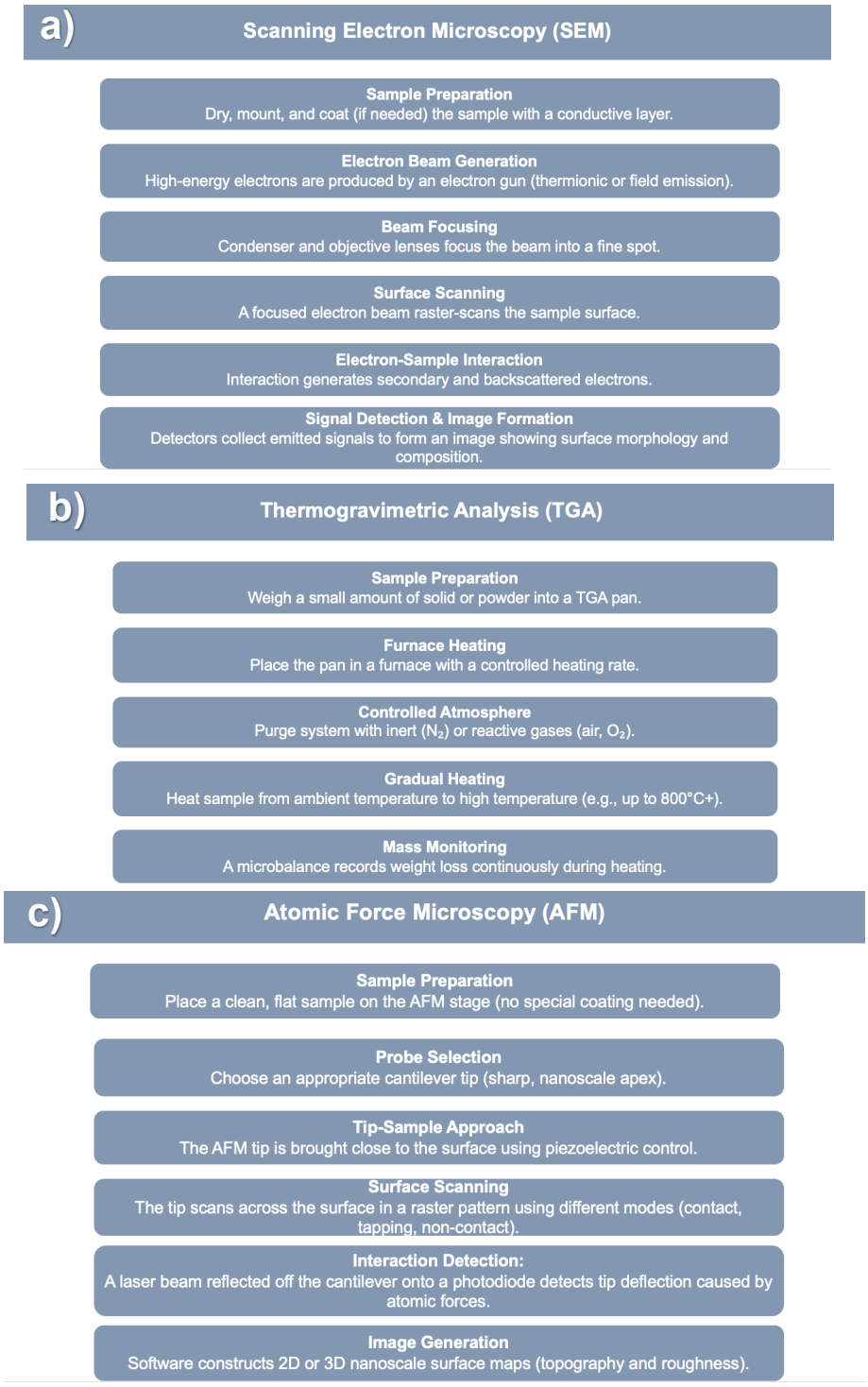

Fig. 11. Characterization techniques for material analysis.

4.1. Synthesis reproducibility and scale-up

One of the foremost challenges is achieving reproducible synthesis and reliable scale-up. Conventional methods, such as co-precipitation, sol–gel, thermal decomposition, and microemulsion, are highly sensitive to slight variations in reaction conditions, including pH, temperature, surfactant concentration, and precursor purity. These parameters significantly influence the particle size, crystallinity, and surface properties of IONPs, resulting in considerable variability between batches. Such inconsistency not only complicates

the transition from laboratory-scale experiments to industrial production but also undermines the performance consistency necessary for clinical applications. Researchers must therefore develop standardized protocols and incorporate real-time, in situ monitoring techniques to understand and control the dynamic processes of nucleation and growth. This detailed control would help establish clear relationships between process parameters and nanoparticle properties, facilitating reproducible large-scale production [104].

4.2. Biocompatibility and safety concerns

Despite their promising applications in imaging, drug delivery, and hyperthermia therapy, IONPs present unresolved challenges regarding biocompatibility and safety. The inherent reactivity of iron oxide surfaces can trigger cytotoxicity, undesirable immune responses, and long-term bioaccumulation issues. Surface functionalization techniques, such as coating nanoparticles with biocompatible polymers or biomolecules, have been developed to mitigate these risks. However, the durability and effectiveness of these modifications under physiological conditions remain to be scrutinized. Furthermore, the adoption of green synthesis methods—utilizing plant extracts or microbial processes, while environmentally appealing, introduces additional variability due to the inconsistent composition of natural extracts. A deeper, systematic investigation into the nano-bio interface, including comprehensive in vivo studies, is crucial to establish a robust safety profile that addresses both short-term and long-term exposure concerns [106].

4.3. Advanced characterization techniques

Accurate and comprehensive characterization of IONPs is crucial for correlating their physicochemical properties with biological performance. Traditional methods such as TEM, XRD, DLS, FTIR, and VSM provide valuable insights into morphology, crystallinity, particle size distribution, and magnetic behavior. However, these techniques often offer isolated snapshots rather than a holistic view of the nanoparticle behavior. To fully understand and optimize IONPs, there is a growing need for multidimensional and in situ characterization approaches that can capture real-time dynamics during both synthesis and application. Incorporating computational modeling and machine learning can further enhance predictive capabilities, allowing researchers to simulate and optimize nanoparticle behavior even before experimental validation, thus bridging the gap between theoretical design and practical performance [93].

4.4. Regulatory and translational hurdles

A significant barrier to the clinical translation of IONPs is the complex regulatory environment. Although numerous IONP formulations have shown promising preclinical results, few have successfully navigated the stringent regulatory requirements necessary for clinical approval. This gap is primarily due to the lack of universally accepted standards for nanoparticle synthesis and characterization, resulting in inconsistencies in quality and performance. Moreover, long-term studies addressing the chronic effects of nanoparticle exposure are limited, making it difficult to establish definitive safety profiles. To facilitate clinical translation, there is a pressing need for interdisciplinary collaboration among materials scientists, clinicians, and regulatory bodies. Establishing standardized protocols and conducting rigorous, long-term clinical trials will be pivotal in creating a clear regulatory pathway for IONP-based applications [106].

4.5. Future directions

The future of IONP technology hinges on addressing the multifaceted challenges of synthesis reproducibility, comprehensive characterization, biocompatibility, and regulatory approval. By developing robust, standardized synthesis protocols, enhancing real-time monitoring and multidimensional characterization techniques, and undertaking extensive safety and efficacy studies, the next generation of IONPs can be engineered for improved performance and safety. These advancements will pave the way for the reliable, scalable production of high-quality nanoparticles, ultimately accelerating their clinical adoption and expanding their applications across various industrial domains. This integrated approach is essential for unlocking the full potential of IONPs in advancing nanomedicine and related fields [107].

CRediT authorship contribution statement

Saad Ahmed: Conceptualization, Methodology, Visualization, Writing – original draft, Writing – review & editing.
Seema Inayat: Visualization, Supervision, Writing – original draft, Writing – review & editing.
Iram Javed: Validation, Writing – review & editing.

Data availability

No new data were generated or analyzed in support of this study.

Declaration of competing interest

The authors declare no competing interests.

Funding and acknowledgment

No funding from any public, commercial, or not-for-profit sector was involved in this review, and the authors have no acknowledgments to declare.

References

[1] S. Malik, K. Muhammad, Y. Waheed, Nanotechnology: A Revolution in Modern Industry, Molecules. 28 (2023) 661. https://doi.org/10.3390/molecules28020661.
[2] S.F. Medeiros, A.M. Santos, H. Fessi, A. Elaissari, Stimuli-responsive magnetic particles for biomedical applications, Int. J. Pharm. 403 (2011) 139–161. https://doi.org/10.1016/j.ijpharm.2010.10.011.
[3] B. Chen, Daunorubicin-Loaded Magnetic Nanoparticles of Fe3O4 Overcome Multidrug Resistance and Induce Apoptosis of K562-n/VCR Cells in Vivo, Int. J. Nanomed. 4 (2009) 201–208. https://doi.org/10.2147/ijn.s7287.
[4] M. Salehirozveh, P. Dehghani, I. Mijakovic, Synthesis, Functionalization, and Biomedical Applications of Iron Oxide

Nanoparticles (IONPs), J. Func. Biomater. 15 (2024) 340–340. https://doi.org/10.3390/jfb15110340.
[5] A. Ali, H. Zafar, M. Zia, I. ul Haq, A.R. Phull, et al., Synthesis, characterization, applications, and challenges of iron oxide nanoparticles, Nanotechnol. Sci. Appl. 9 (2016) 49–67. https://doi.org/10.2147/nsa.s99986.
[6] C.-T. Wang, S.-H. Ro, Nanocluster Iron Oxide-Silica Aerogel Catalysts for Methanol Partial Oxidation, Appl. Catal. A: Gen. 285 (2005) 196–204. https://doi.org/10.1016/j.apcata.2005.02.029.
[7] A.K. Gupta, M. Gupta, Synthesis and Surface Engineering of Iron Oxide Nanoparticles for Biomedical Applications, Biomaterials. 26 (2005) 3995–4021. https://doi.org/10.1016/j.biomaterials.2004.10.012.
[8] J. Estelrich, E. Escribano, J. Queralt, M. Busquets, Iron Oxide Nanoparticles for Magnetically-Guided and Magnetically-Responsive Drug Delivery, Int. J. Mol. Sci. 16 (2015) 8070–8101. https://doi.org/10.3390/ijms16048070.
[9] K.G. Gareev, Diversity of Iron Oxides: Mechanisms of Formation, Physical Properties and Applications, Magnetochemistry. 9 (2023) 119–119. https://doi.org/10.3390/magnetochemistry9050119.
[10] T.R. Kyriakides, A. Raj, T.H. Tseng, H. Xiao, R. Nguyen, et al., Biocompatibility of nanomaterials and their immunological properties, Biomed. Mater. 16 (2021) 042005. https://doi.org/10.1088/1748-605X/abe5fa.
[11] R. Agarwal, S. Adhikary, S. Bhattacharya, S. Goswami, D. Roy, et al., The Iron Oxide Nanoparticles: A Narrative Review of In-depth Analysis from Neuroprotection to Neurodegeneration, Environ. Sci. Adv. 3 (2024) 635–660. https://doi.org/10.1039/d4va00062e.
[12] W. Wu, Z. Wu, T. Yu, C. Jiang, W.-S. Kim, Recent Progress on Magnetic Iron Oxide Nanoparticles: Synthesis, Surface Functional Strategies and Biomedical Applications, Sci. Technol. Adv. Mater. 16 (2015) 023501. https://doi.org/10.1088/1468-6996/16/2/023501.
[13] N. Ajinkya, X. Yu, P. Kaithal, H. Luo, P. Somani, S. Ramakrishna, Magnetic Iron Oxide Nanoparticle (IONP) Synthesis to Applications: Present and Future, Materials. 13 (2020) 4644. https://doi.org/10.3390/ma13204644.
[14] Wahajuddin, S. Arora, Superparamagnetic Iron Oxide Nanoparticles: Magnetic Nanoplatforms as Drug Carriers, Int. J. Nanomed. 7 (2012) 3445–3471. https://doi.org/10.2147/IJN.S30320.
[15] B.E. Keshta, A.H. Gemeay, D.K. Sinha, S. Elsharkawy, F. Hassan, et al., State of the Art on the Magnetic Iron Oxide Nanoparticles: Synthesis, Functionalization, and Applications in Wastewater Treatment, Results Chem. 7 (2024) 101388–101388. https://doi.org/10.1016/j.rechem.2024.101388.
[16] N. Lee, T. Hyeon, Designed synthesis of uniformly sized iron oxide nanoparticles for efficient magnetic resonance imaging contrast agents, Chem. Soc. Rev. 41 (2012) 2575–2589. https://doi.org/10.1039/c1cs15248c.
[17] A.P. Khandhar, R.M. Ferguson, H. Arami, K.M. Krishnan, Monodisperse Magnetite Nanoparticle Tracers for in Vivo Magnetic Particle Imaging, Biomaterials. 34 (2013) 3837–3845. https://doi.org/10.1016/j.biomaterials.2013.01.087.
[18] H. Xu, L. Cheng, C. Wang, X. Ma, Y. Li, Z. Liu, Polymer encapsulated upconversion nanoparticle/iron oxide nanocomposites for multimodal imaging and magnetic targeted drug delivery, Biomaterials. 32 (2011) 9364–9373. https://doi.org/10.1016/j.biomaterials.2011.08.053.
[19] J. Mccarthy, R. Weissleder, Multifunctional Magnetic Nanoparticles for Targeted Imaging and Therapy, Adv. Drug Deliv. Rev. 60 (2008) 1241–1251. https://doi.org/10.1016/j.addr.2008.03.014.
[20] N. Schleich, F. Danhier, V. Préat, Iron oxide-loaded nanotheranostics: Major obstacles to in vivo studies and clinical translation, J. Contr. Release. 198 (2015) 35–54. https://doi.org/10.1016/j.jconrel.2014.11.024.
[21] M. Mahmoudi, S. Sant, B. Wang, S. Laurent, T. Sen, Superparamagnetic iron oxide nanoparticles (SPIONs): Development, surface modification and applications in chemotherapy, Adv. Drug Deliv. Rev. 63 (2011) 24–46. https://doi.org/10.1016/j.addr.2010.05.006.
[22] E.A. Périgo, G. Hemery, O. Sandre, D. Ortega, E. Garaio, F. Plazaola, F.J. Teran, Fundamentals and advances in magnetic hyperthermia, Appl. Phys. Rev. 2 (2015) 041302. https://doi.org/10.1063/1.4935688.
[23] J.B. Haun, T.-J. Yoon, H. Lee, R. Weissleder, Magnetic nanoparticle biosensors, Wiley Interdiscip. Rev. Nanomed. Nanobiotechnol. 2 (2010) 291–304. https://doi.org/10.1002/wnan.84.
[24] K. Salahuddin Siddiqi, A. ur Rahman, Tajuddin, A. Husen, Biogenic Fabrication of Iron/Iron Oxide Nanoparticles and Their Application, Nanoscale Res. Lett. 11 (2016) 498. https://doi.org/10.1186/s11671-016-1714-0.
[25] S.C. Tan, B.C. Yiap, DNA, RNA, and Protein Extraction: The Past and The Present, J. Biomed. Biotechnol. 2009 (2009) 1–10. https://doi.org/10.1155/2009/574398.
[26] M.W. Mazhar, M. Ishtiaq, M. Maqbool, R. Akram, A. Shahid, et al., Seed Priming with Iron Oxide Nanoparticles Raises Biomass Production and Agronomic Profile of Water-Stressed Flax Plants, Agronomy. 12 (2022) 982–982. https://doi.org/10.3390/agronomy12050982.
[27] T. Assefa Aragaw, F. Mazengiaw Bogale, B. Asefa Aragaw, Iron-Based Nanoparticles in Wastewater Treatment: A Review on Synthesis Methods, Applications, and Removal Mechanisms, J. Saudi Chem. Soc. 25 (2021) 101280. https://doi.org/10.1016/j.jscs.2021.101280.
[28] O. Gohar, M. Zubair Khan, I. Bibi, N. Bashir, U. Tariq, et al., Nanomaterials for Advanced Energy Applications: Recent Advancements and Future Trends, Mater. Design. 241 (2024) 112930–112930. https://doi.org/10.1016/j.matdes.2024.112930.
[29] Y. Gao, L. Shao, S. Yang, J. Hu, S. Zhao, et al., Recent advances in iron-based catalysts for Fischer–Tropsch to olefins reaction, Catal. Commun. 181 (2023) 106720. https://doi.org/10.1016/j.catcom.2023.106720.
[30] L. Xuan, Z. Ju, M. Skonieczna, P.K. Zhou, R. Huang, Nanoparticles-induced potential toxicity on human health: Applications, toxicity mechanisms, and evaluation models, MedComm. 4 (2023) e327. https://doi.org/10.1002/mco2.327.
[31] S. Laurent, D. Forge, M. Port, A. Roch, C. Robic, et al., Magnetic iron oxide nanoparticles: synthesis, stabilization, vectorization, physicochemical characterizations, and biological applications, Chem. Rev. 108 (2008) 2064–2110. https://doi.org/10.1021/cr068445e.
[32] T. Ahn, J.H. Kim, H.-M. Yang, J.W. Lee, J.-D. Kim, Formation Pathways of Magnetite Nanoparticles by Coprecipitation Method, J. Phys. Chem. C. 116 (2012) 6069–6076. https://doi.org/10.1021/jp211843g.
[33] G. Gnanaprakash, S. Mahadevan, T. Jayakumar, P. Kalyanasundaram, J. Philip, B. Raj, Effect of Initial pH and Temperature of Iron Salt Solutions on Formation of Magnetite Nanoparticles, Mater. Chem. Phys. 103 (2007) 168–175. https://doi.org/10.1016/j.matchemphys.2007.02.011.
[34] N.T.K. Thanh, N. Maclean, S. Mahiddine, Mechanisms of Nucleation and Growth of Nanoparticles in Solution, Chem. Rev. 114 (2014) 7610–7630. https://doi.org/10.1021/cr400544s.
[35] R.A. Harris, P.M. Shumbula, H. van der Walt, Analysis of the Interaction of Surfactants Oleic Acid and Oleylamine with Iron Oxide Nanoparticles through Molecular Mechanics Modeling, Langmuir. 31 (2015) 3934–3943. https://doi.org/10.1021/acs.langmuir.5b00671.
[36] J. Choi, B. Hyo Kim, Ligands of Nanoparticles and Their Influence on the Morphologies of Nanoparticle-Based Films, Nanomaterials. 14 (2024) 1685–1685. https://doi.org/10.3390/nano14201685.
[37] D. José Pochapski, C. Carvalho dos Santos, G. Wosiak Leite, S. Helena Pulcinelli, C. Valentim Santilli, Zeta Potential and Colloidal Stability Predictions for Inorganic Nanoparticle Dispersions: Effects of Experimental Conditions and Electrokinetic Models on the

Interpretation of Results, Langmuir. 37 (2021) 13379–13389. https://doi.org/10.1021/acs.langmuir.1c02056.
[38] H. Ohshima, DLVO theory of colloid stability, Interface Science and Technology, Elsevier. 37 (2024) 217–244. https://doi.org/10.1016/b978-0-443-16116-2.00009-6.
[39] G.J. Owens, R.K. Singh, F. Foroutan, M. Alqaysi, C.-M. Han, et al., Sol–Gel Based Materials for Biomedical Applications, Prog. Mater. Sci. 77 (2016) 1–79. https://doi.org/10.1016/j.pmatsci.2015.12.001.
[40] N. Baig, I. Kammakakam, W. Falath, Nanomaterials: A Review of Synthesis Methods, Properties, Recent Progress, and Challenges, Mater. Adv. 2 (2021) 1821–1871. https://doi.org/10.1039/d0ma00807a.
[41] L. Durães, O. Oliveira, L. Benedini, B.F.O. Costa, A.M. Beja, A. Portugal, Sol–gel Synthesis of Iron(III) Oxyhydroxide Nanostructured Monoliths Using Fe(NO3)3·9H2O/CH3CH2OH/NH4OH Ternary System, J. Phys. Chem. Solids. 72 (2011) 678–684. https://doi.org/10.1016/j.jpcs.2011.02.020.
[42] D. Bokov, A. Turki Jalil, S. Chupradit, W. Suksatan, M. Javed Ansari, et al., Nanomaterial by Sol-Gel Method: Synthesis and Application, Adv. Mater. Sci. Eng. 2021 (2021) 1–21. https://doi.org/10.1155/2021/5102014.
[43] S. Sopan Mahato, D. Mahata, S. Panda, M. Shrabani, Perspective Chapter: Sol-Gel Science and Technology in Context of Nanomaterials – Recent Advances, IntechOpen. (2023). https://doi.org/10.5772/intechopen.111378.
[44] S. Esposito,"Traditional" Sol-Gel Chemistry as a Powerful Tool for the Preparation of Supported Metal and Metal Oxide Catalysts, Materials. 12 (2019) 668. https://doi.org/10.3390/ma12040668.
[45] D. Navas, S. Fuentes, A. Castro-Alvarez, E. Chavez-Angel, Review on Sol-Gel Synthesis of Perovskite and Oxide Nanomaterials, Gels. 7 (2021) 275. https://doi.org/10.3390/gels7040275.
[46] K. Nishio, T. Tsuchiya, Sol-Gel Processing of Thin Films with Metal Salts, Springer. (2018) 133–154. https://doi.org/10.1007/978-3-319-32101-1_3.
[47] S. Stankic, S. Suman, F. Haque, J. Vidic, Pure and multi metal oxide nanoparticles: synthesis, antibacterial and cytotoxic properties, J. Nanobiotechnol. 14 (2016) 73. https://doi.org/10.1186/s12951-016-0225-6.
[48] T. Coradin, Sol-Gel Process, Structure, and Properties, Handbook of Cell Biosensors, Springer, Cham. (2021) 497–516. https://doi.org/10.1007/978-3-030-23217-7_141.
[49] M. Fatima, S. Riaz, Z.N. Kayani, S. Naseem, Effect of Calcination on Phase Transition in Iron Oxide Nanoparticles, Mater. Today: Proceed. 2 (2015) 5743–5747. https://doi.org/10.1016/j.matpr.2015.11.120.
[50] T. Takiya, K. Furukawa, N. Fukuda, M. Han, M. Yaga, Nucleation Kinetics, Size Effects, and Surface Treatment, Handbook of Nanoparticles, Springer, Cham. (2015) 245–264. https://doi.org/10.1007/978-3-319-15338-4_15.
[51] C.R. O'Melia, Fundamentals of particle stability, Interface Sci. Technol. 10 (2006) 317–362. https://doi.org/10.1016/s1573-4285(06)80087-6.
[52] S. Sun, H. Zeng, Size-Controlled Synthesis of Magnetite Nanoparticles, J. Am. Chem. Soc. 124 (2002) 8204–8205. https://doi.org/10.1021/ja026501x.
[53] T. Hyeon, S. Seong Lee, J. Park, Y. Chung, H. Bin Na, Synthesis of Highly Crystalline and Monodisperse Maghemite Nanocrystallites without a Size-Selection Process, J. Am. Chem. Soc. 123 (2001) 12798–12801. https://doi.org/10.1021/ja016812s.
[54] A. Nyabadza, É. McCarthy, M.A. Makhesana, S. Heidarinassab, A. Plouze, M. Vázquez, D. Brabazon, A Review of Physical, Chemical and Biological Synthesis Methods of Bimetallic Nanoparticles and Applications in Sensing, Water Treatment, Biomedicine, Catalysis and Hydrogen Storage, Adv. Colloid Interface Sci. 321 (2023) 103010–103010. https://doi.org/10.1016/j.cis.2023.103010.
[55] M. Unni, A.M. Uhl, S. Savliwala, B.H. Savitzky, R. Dhavalikar, et al., Thermal Decomposition Synthesis of Iron Oxide Nanoparticles with Diminished Magnetic Dead Layer by Controlled Addition of Oxygen, ACS Nano. 11 (2017) 2284–2303. https://doi.org/10.1021/acsnano.7b00609.
[56] A. Lassenberger, T.A. Grünewald, P.D.J. van Oostrum, H. Rennhofer, H. Amenitsch, et al., Monodisperse Iron Oxide Nanoparticles by Thermal Decomposition: Elucidating Particle Formation by Second-Resolved in Situ Small-Angle X-ray Scattering, Chem. Mater. 29 (2017) 4511–4522. https://doi.org/10.1021/acs.chemmater.7b01207.
[57] H. Heinz, C. Pramanik, O. Heinz, Y. Ding, R.K. Mishra, et al., Nanoparticle decoration with surfactants: Molecular interactions, assembly, and applications, Surface Sci. Rep. 72 (2017) 1–58. https://doi.org/10.1016/j.surfrep.2017.02.001.
[58] G. Murali Manoj, M. Shalini, K. Thenmozhi, V.K. Ponnusamy, S. Hari, Recent advancements in the surface modification and functionalization of magnetic nanomaterials, Appl. Surface Sci. Adv. 21 (2024) 100608–100608. https://doi.org/10.1016/j.apsadv.2024.100608.
[59]C. Okoli, M. Sanchez-Dominguez, M. Boutonnet, S. Järås, C. Civera, et al., Comparison and Functionalization Study of Microemulsion-Prepared Magnetic Iron Oxide Nanoparticles, Langmuir. 28 (2012) 8479–8485. https://doi.org/10.1021/la300599q.
[60] M.A. Malik, M.Y. Wani, M.A. Hashim, Microemulsion method: A novel route to synthesize organic and inorganic nanomaterials, Arab. J. Chem. 5 (2012) 397–417. https://doi.org/10.1016/j.arabjc.2010.09.027.
[61] O. Glatter, S. Salentinig, Inverting Structures: from Micelles via Emulsions to Internally Self-assembled Water and Oil Continuous Nanocarriers, Curr. Opin. Colloid Interface Sci. 49 (2020) 82–93. https://doi.org/10.1016/j.cocis.2020.05.003.
[62] P. Taylor, Ostwald Ripening in Emulsions, Adv. Colloid Interface Sci. 75 (1998) 107–163. https://doi.org/10.1016/s0001-8686(98)00035-9.
[63] P. Baláž, Mechanochemistry in Nanoscience and Minerals Engineering, Springer, Berlin Heidelberg. (2008). https://doi.org/10.1007/978-3-540-74855-7.
[64] C. Suryanarayana, Mechanical Alloying and Milling, Prog. Mater. Sci. 46 (2001) 1–184. https://doi.org/10.1016/s0079-6425(99)00010-9.
[65] H. Sun, L. Wei, Y. Zuo, Y. Wu, Effective separation and simultaneous detection of gatifloxacin, aminomethylbenzoic acid, cefazolin and cefminox in human urine by capillary zone electrophoresis, J. Iran. Chem. Soc. 8 (2011) 1043–1051. https://doi.org/10.1007/bf03246561.
[66] N. de Vries, X. Zhu, E.R. Kieft, J. van der Mullen, Time resolved Thomson scattering measurements on a high pressure mercury lamp, J. Phys. D: Appl. Phys. 38 (2005) 2778–2789. https://doi.org/10.1088/0022-3727/38/16/006.
[67] V. Amendola, M. Meneghetti, Laser Ablation Synthesis in Solution and Size Manipulation of Noble Metal Nanoparticles, Phys. Chem. Chem. Phys. 11 (2009) 3805–3821. https://doi.org/10.1039/b900654k.
[68] S. Barcikowski, A. Hahn, A.V. Kabashin, B.N. Chichkov, Properties of nanoparticles generated during femtosecond laser machining in air and water, Appl. Phys. A. 87 (2007) 47–55. https://doi.org/10.1007/s00339-006-3852-1.
[69]M.J. Ansari, M.M. Kadhim, B. Abed Hussein, H.A. Lafta, E. Kianfar, Synthesis and Stability of Magnetic Nanoparticles, BioNanoScience. 12 (2022) 627–638. https://doi.org/10.1007/s12668-022-00947-5.
[70] S. Hosseynizadeh Khezri, A. Yazdani, R. Khordad, Pure Iron Nanoparticles Prepared by Electric Arc Discharge Method in Ethylene Glycol, Eur. Phys. J. Appl. Phys. 59 (2012) 30401. https://doi.org/10.1051/epjap/2012110303.

[71] M. Lahav, T. Sehayek, A. Vaskevich, I. Rubinstein, Nanoparticle Nanotubes, Angew. Chem. Int. Ed. 42 (2003) 5576–5579. https://doi.org/10.1002/anie.200352216.
[72] D. Escorcia-Díaz, S. García-Mora, L. Rendón-Castrillón, M. Ramírez-Carmona, C. Ocampo-López, Advancements in Nanoparticle Deposition Techniques for Diverse Substrates: A Review, Nanomaterials. 13 (2023) 2586–2586. https://doi.org/10.3390/nano13182586.
[73] B.K. Ozcelik, C. Ergun, Synthesis and Characterization of Iron Oxide Particles Using Spray Pyrolysis Technique, Ceram. Int. 41 (2014) 1994–2005. https://doi.org/10.1016/j.ceramint.2014.09.103.
[74] S. Kazemi, A. Hosseingholian, S.D. Gohari, F. Feirahi, F. Moammeri, et al., Recent Advances in Green Synthesized Nanoparticles: From Production to Application, Mater. Today Sustain. 24 (2023) 100500. https://doi.org/10.1016/j.mtsust.2023.100500.
[75] R.N. Morgan, K.M. Aboshanab, Green biologically synthesized metal nanoparticles: biological applications, optimizations and future prospects, Future Sci. OA. 10 (2024) FSO935. https://doi.org/10.2144/fsoa-2023-0196.
[76] M. Thatyana, N.P. Dube, D. Kemboi, A.E. Manicum, N.S. Mokgalaka-Fleischmann, J.V. Tembu, Advances in Phytonanotechnology: A Plant-Mediated Green Synthesis of Metal Nanoparticles Using Phyllanthus Plant Extracts and Their Antimicrobial and Anticancer Applications, Nanomaterials (Basel). 13 (2023) 2616. https://doi.org/10.3390/nano13192616.
[77] A. Ebrahiminezhad, A. Zare-Hoseinabadi, A.K. Sarmah, S. Taghizadeh, Y. Ghasemi, A. Berenjian, Plant-Mediated Synthesis and Applications of Iron Nanoparticles, Mol. Biotechnol. 60 (2017) 154–168. https://doi.org/10.1007/s12033-017-0053-4.
[78] A. Fariq, T. Khan, A. Yasmin, Microbial Synthesis of Nanoparticles and Their Potential Applications in Biomedicine, J. Appl. Biomed. 15 (2017) 241–248. https://doi.org/10.1016/j.jab.2017.03.004.
[79] B. Koul, A. Kumar Poonia, D. Yadav, J.-O. Jin, Microbe-Mediated Biosynthesis of Nanoparticles: Applications and Future Prospects, Biomolecules. 11 (2021) 886. https://doi.org/10.3390/biom11060886.
[80] G. Grasso, D. Zane, R. Dragone, Microbial Nanotechnology: Challenges and Prospects for Green Biocatalytic Synthesis of Nanoscale Materials for Sensoristic and Biomedical Applications, Nanomaterials. 10 (2020) 11. https://doi.org/10.3390/nano10010011.
[81] P. Singh, Y.-J. Kim, D. Zhang, D.-C. Yang, Biological Synthesis of Nanoparticles from Plants and Microorganisms, Trends Biotechnol. 34 (2016) 588–599. https://doi.org/10.1016/j.tibtech.2016.02.006.
[82]D. Fawcett, J.J. Verduin, M. Shah, S.B. Sharma, G. Eddy Jai Poinern, A Review of Current Research into the Biogenic Synthesis of Metal and Metal Oxide Nanoparticles via Marine Algae and Seagrasses, J. Nanosci. 2017 (2017) 8013850. https://doi.org/10.1155/2017/8013850.
[83] T. Nagamune, Biomolecular Engineering for Nanobio/bionanotechnology, Nano Converg. 4 (2017) 9. https://doi.org/10.1186/s40580-017-0103-4.
[84] A.F. Kareemi, S, Likhitkar, Applications and Advancements of Polysaccharide-Based Nanostructures for Enhanced Drug Delivery, Colloids Surf. B: Biointerfaces. 238 (2024) 113883–113883. https://doi.org/10.1016/j.colsurfb.2024.113883.
[85] C. Pechyen, B. Tangnorawich, S. Toommee, R. Marks, Y. Parcharoen, Green Synthesis of Metal Nanoparticles, Characterization, and Biosensing Applications, Sensors Int. 5 (2024) 100287–100287. https://doi.org/10.1016/j.sintl.2024.100287.
[86] N.S. Al-Radadi, Microwave assisted green synthesis of Fe@Au core–shell NPs magnetic to enhance olive oil efficiency on eradication of helicobacter pylori (life preserver), Arab. J. Chem. 15 (2022) 103685–103685. https://doi.org/10.1016/j.arabjc.2022.103685.
[87] T.P. Huelser, H. Wiggers, P. Ifeacho, O. Dmitrieva, G. Dumpich, A. Lorke, Morphology, Structure and Electrical Properties of Iron Nanochains, Nanotechnology. 17 (2006) 3111–3115. https://doi.org/10.1088/0957-4484/17/13/005.
[88] M. Asadi Asadabad, M. Jafari Eskandari, Transmission Electron Microscopy as Best Technique for Characterization in Nanotechnology, Synth. React. Inorg. Met.-Org. Nano-Met. Chem. 45 (2014) 323–326. https://doi.org/10.1080/15533174.2013.831901.
[89] S.I. Ali Shah, W. Ahmad, M. Anwar, R. Shah, J. Ali Khan, et al., Synthesis, Properties, and Applications of Fe3O4 and Fe3O4-Based Nanocomposites: A Review, Appl. Catal. O: Open. 203 (2025) 207049. https://doi.org/10.1016/j.apcato.2025.207049.
[90] B. Wu, L.-J. Zhang, C.-J. Zhang, K. Deng, Y.-W. Ao, et al., Effect of Poly(ethylene glycol) (PEG) Surface Density on the Fate and Antitumor Efficacy of Redox-Sensitive Hybrid Nanoparticles, ACS Biomater. Sci. Eng. 6 (2020) 3975–3983. https://doi.org/10.1021/acsbiomaterials.0c00516.
[91] S. Mourdikoudis, R.M. Pallares, N.T.K. Thanh, Characterization techniques for nanoparticles: comparison and complementarity upon studying nanoparticle properties, Nanoscale. 10 (2018) 12871–12934. https://doi.org/10.1039/c8nr02278j.
[92] H. Shagholani, S.M. Ghoreishi, M. Mousazadeh, Improvement of the Interaction between PVA and Chitosan via Magnetite Nanoparticles for Drug Delivery Applications, Int. J. Biol. Macromol. 78 (2015) 130–136. https://doi.org/10.1016/j.ijbiomac.2015.02.042.
[93] S. Sharma, S.K. Shukla, K.K. Govender, P.P. Govender, Unveiling the Multifunctionality of Iron Oxide Nanoparticle: A Synergistic Experimental and Computational Investigation, Chem. Phys. Impact. 10 (2025) 100845. https://doi.org/10.1016/j.chphi.2025.100845.
[94] J. Stetefeld, S.A. McKenna, T.R. Patel, Dynamic Light Scattering: A Practical Guide and Applications in Biomedical Sciences, Biophys. Rev. 8 (2016) 409–427. https://doi.org/10.1007/s12551-016-0218-6.
[95] J. Jia, J. Li, L. Gao, D. Yang, A. Kanaev, Dynamic Light Scattering: A Powerful Tool for In Situ Nanoparticle Sizing, Colloids Interfaces. 7 (2023) 15. https://doi.org/10.3390/colloids7010015.
[96] M.M. Eid, Characterization of Nanoparticles by FTIR and FTIR-Microscopy, Handbook of Consumer Nanoproducts, Springer, Singapore. (2022) 645–673. https://doi.org/10.1007/978-981-16-8698-6_89.
[97] D. Khadka, P. Gautam, R. Dahal, M.D. Ashie, H. Paudyal, et al., Evaluating the Photocatalytic Activity of Green Synthesized Iron Oxide Nanoparticles, Catalysts. 14 (2024) 751–751. https://doi.org/10.3390/catal14110751.
[98] O. Karaagac, H. Köçkar, Improvement of the Saturation Magnetization of PEG Coated Superparamagnetic Iron Oxide Nanoparticles, J. Magn. Magn. Mater. 551 (2022) 169140–169140. https://doi.org/10.1016/j.jmmm.2022.169140.
[99] N.D.S. Zambri, N.I. Taib, F. Abdul Latif, Z. Mohamed, Utilization of Neem Leaf Extract on Biosynthesis of Iron Oxide Nanoparticles, Molecules. 24 (2019) 3803. https://doi.org/10.3390/molecules24203803.
[100] S.E. Sandler, B. Fellows, O. Thompson Mefford, Best Practices for Characterization of Magnetic Nanoparticles for Biomedical Applications, Anal. Chem. 91 (2019) 14159–14169. https://doi.org/10.1021/acs.analchem.9b03518.
[101] C. Pucci, A. Degl'Innocenti, M. Belenli Gümüş, G. Ciofani, Superparamagnetic Iron Oxide Nanoparticles for Magnetic Hyperthermia: Recent Advancements, Molecular Effects, and Future Directions in the Omics Era, Biomater. Sci. 10 (2022) 2103–2121. https://doi.org/10.1039/d1bm01963e.
[102] S.M. Dadfar, D. Camozzi, M. Darguzyte, K. Roemhild, P. Varvarà, et al., Size-isolation of superparamagnetic iron oxide nanoparticles improves MRI, MPI and hyperthermia performance, J. Nanobiotechnol. 18 (2020) 22. https://doi.org/10.1186/s12951-020-05801.
[103] M. Arif, H. Raza, T. Akhter, UV-Vis Spectroscopy in the Characterization and Applications of Smart Microgels and Metal Nanoparticle-Decorated Smart Microgels: A Critical Review, RSC Adv. 14 (2024) 38120–38134. https://doi.org/10.1039/d4ra07643e.

[104] A. Baki, F. Wiekhorst, R. Bleul, Advances in Magnetic Nanoparticles Engineering for Biomedical Applications—A Review, Bioengineering. 8 (2021) 134. https://doi.org/10.3390/bioengineering8100134.

[105] A.G. Leonel, A.A.P. Mansur, H.S. Mansur, Nanotoxicity and Environmental Risks of Magnetic Iron Oxide Nanoparticles and Nanohybrids, Handbook of Magnetic Hybrid Nanoalloys and their Nanocomposites, Springer, Cham. (2022) https://doi.org/10.1007/978-3-030-90948-2_36.

[106] R. Ghazi, T.K. Ibrahim, J.A. Nasir, S. Gai, G. Ali, et al., Iron oxide based magnetic nanoparticles for hyperthermia, MRI and drug delivery applications: a review. RSC Adv. 15 (2025) 11587–11616. https://doi.org/10.1039/d5ra00728c.

[107] S. Ahmed, Nanotechnology and Biotechnology Against Multidrug-Resistant Pathogens: Promises and Challenges, Exon. 2 (2025) 152–164. https://doi.org/10.69936/en09y0025.